ACS OMEGA

Open Access

This article is licensed under CC-BY-NC-ND 4.0

http://pubs.acs.org/journal/acsodf

Review

# Application of Refrigerant Cooling in a Battery Thermal Management System under High Temperature Conditions: A Review

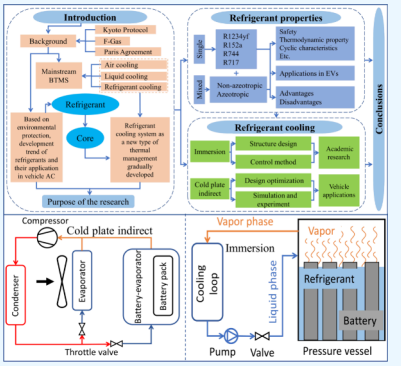
Yujia Kang, Yunpeng Hu,* Chunhua Zhang,* Ke Yang, and Quan Zhang

Cite This: *ACS Omega* 2024, 9, 25591−25609

Read Online

ACCESS | Metrics & More | Article Recommendations

**ABSTRACT:** Battery thermal management (BTM) is crucial for the lifespan and safety of batteries. Refrigerant cooling is a novel cooling technique that is being used gradually. As the core fluid of refrigerant cooling, refrigerants need to possess excellent properties while meeting environmental requirements. This paper elucidates the current state of refrigerants (single refrigerants and mixed refrigerants), synchronously summarizing them from the perspectives of refrigerant properties and refrigerant cooling (immersion and cold plate indirect). It outlines the advantages and disadvantages of single and mixed refrigerants as well as the research and development in the vehicle thermal management system (TMS). The choice of refrigerant directly affects cooling performance, and research on vehicle air conditioning (AC) systems can indirectly guide the BTM. R1234yf and R152a can directly replace R134a, while although R744 has a strong heating capacity, it cannot directly replace R134a. Specific mixed refrigerants reduce the global warming potential (GWP) and flammability issues, thereby improving system efficiency. Additionally, immersion cooling controls the temperature through container pressure. Coordinated control strategies are crucial for indirect cold plate cooling, offering broad prospects for optimizing the cold plate design and intelligent control. The selection of refrigerant and the optimal design of the cooling method greatly improve the thermal performance of the battery. This may promote the good development of BTM.




Downloaded via 188.119.36.123 on November 29, 2025 at 13:03:03 (UTC).
See https://pubs.acs.org/sharingguidelines for options on how to legitimately share published articles.

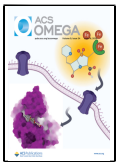
## 1. INTRODUCTION

In the new era, emissions from industry and fuel consumption often cause serious environmental problems.[1] In order to reduce $CO_2$ and greenhouse gas emissions and at the same time ease the consumption of fossil fuels as the main energy source,[2] governments of various countries actively promote the development and application of green and renewable energy such as solar energy, wind energy, and water energy.[3] In addition, as a newly developing type of transportation, electric vehicles (EVs) have the characteristics of "zero emission" and are also considered to be one of the effective ways to reduce fossil energy consumption.

The Chinese Government has set forth the objective of reaching the peak of carbon emissions by 2030 and attaining carbon neutrality by 2060 in alignment with global initiatives focused on energy conservation and emission reduction.[4] EVs have gradually replaced traditional fuel vehicles, and the global stock of EVs has been increasing year by year, with production and sales volumes showing a significant upward trend.[5] As of the end of 2022, the stock of new energy vehicles (NEVs) reached 13.1 million, representing approximately 4.10% of the total vehicle population, an increase of 67.13% over 2021 after deducting scrapped and deregistered vehicles in China.[6] However, the development of EVs is mainly restricted by power battery. Lithium-ion batteries have gained widespread adoption due to their remarkable energy density and cycle life characteristics.

The optimal operating temperature for lithium-ion batteries ranges from 15 to 35 °C.[7] An adequate thermal management system (TMS) plays a crucial role in the development of EVs.[8,9] Concerning safety, battery overheating may lead to fires or damage the internal structure of the battery. Regarding performance stability, temperature significantly affects the battery performance and lifespan.[10] Overheating reduces the battery performance and accelerates its degradation, thereby shortening its lifespan. Both excessively high and low temperatures affect the battery charging efficiency, resulting in increased energy loss.[11,12] A proper TMS aids in maximizing energy storage and release, enhancing the driving range and overall endurance of EVs.[13] Unfavorable temperature circumstances may cause a significant decrease in battery performance, which would lower the vehicle range.

**Received:** March 26, 2024
**Revised:** May 13, 2024
**Accepted:** May 23, 2024
**Published:** June 5, 2024



© 2024 The Authors. Published by American Chemical Society

**Table 1. Mainstream BTM**

| BTM | advantages | disadvantages | main products |
|---|---|---|---|
| Air cooling | Simple, low cost | Low heat dissipation efficiency | Toyota Prius, KIA Soul EV, etc. |
| Liquid cooling | High heat dissipation efficiency, precise temperature control | Complex, high installation and maintenance costs | Tesla Model 3, GM Volt, GEELY Emgrand EV, VW ID4, etc. |
| Refrigerant cooling | Higher cooling efficiency than liquid cooling, small size, lightweight | Temperature is difficult to control | BMW i3, BYD dolphin, BYD Han-dmi, etc. |

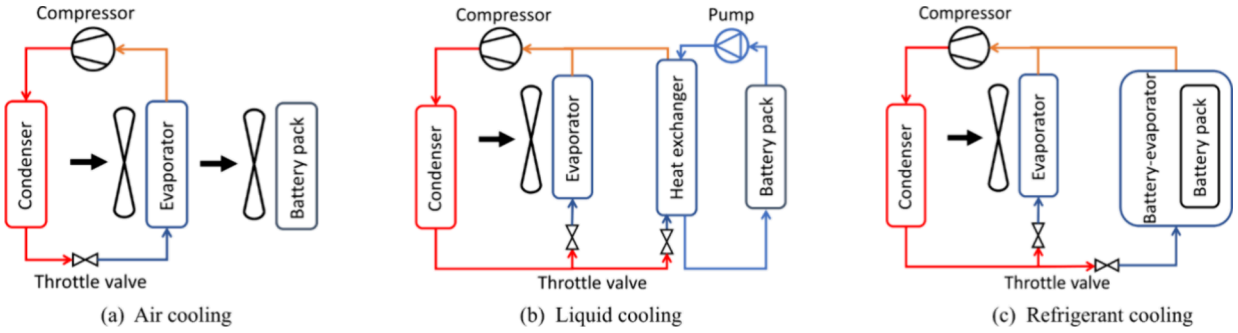



**Figure 1.** (a–c) Schematic diagram of common BTM.

Battery thermal management (BTM) is pivotal in EVs.[14] An efficient TMS may enhance the battery efficiency and lifespan while ensuring safe EV safe operation. Consequently, an effective TMS of EV batteries has garnered considerable attention.[15] There are currently multiple methods for BTM, such as air cooling,[16] liquid cooling,[17] phase-change material (PCM) cooling,[18] refrigerant cooling,[19] and hybrid cooling.[20] Air cooling is a simple and economical way of using BTM. Typically, a fan is employed to facilitate the airflow and remove heat from the surface of the battery module. By changing the airflow distribution through baffles,[21] the results show that the maximum temperature and temperature difference are reduced by 3.42 K (6.26%) and 6.4 K (90.78%), respectively, compared with a typical Z-type battery thermal management system (BTMS). This method is simple and economical, but its thermal management effectiveness is greatly influenced by the external environment, making it suitable for low-power battery modules. Liquid cooling is a method of cooling a coolant (coolant usually is 50% ethylene glycol solution) through pipes to contact the surface of the battery module and remove the heat from the battery module. Compared with air cooling, liquid cooling has a more stable thermal management effect but requires additional equipment such as liquid pipelines and pumps. Study points out that under the same conditions, the average battery temperature in the liquid cooling is about 3 °C lower than that of the air cooling.[22] PCM cooling uses materials with phase change characteristics (such as paraffin) to absorb battery heat. When the material undergoes a phase transition from the solid to liquid state, the absorbed heat is taken away. Compared with liquid cooling, PCM cooling has a higher heat capacity and can absorb more heat in a short time but requires some design and material costs. In an EV operating at 3C (C is C-rate, indicating the charge and discharge current with respect to its nominal capacity) hot climate, 10% expanded graphite-composite PCM has excellent thermal characteristics and thermal safety (that is, the temperature difference is less than 5 K).[23] Refrigerant cooling absorbs battery heat through refrigerant evaporation. It has a high heat transfer efficiency, making it suitable for high-power battery modules. Hybrid cooling combines multiple thermal management methods and can comprehensively utilize the advantages of various thermal management methods to achieve better thermal management effectiveness.[24] Scholars[25] study the collaborative heat dissipation of PCM and liquid cooling, and conclude that under the condition of an ambient temperature of 308.15 K, the temperature can be controlled at 313.15 K, and the appropriate coolant flow rate can maximize the thermal performance of the battery pack.

As the first-generation cooling method, air cooling demonstrates significant structural advantages.[26] However, with advancement in battery energy density, stricter temperature control requirements for batteries have emerged. Liquid cooling remains the mainstream method for heat dissipation to date.[27] Under the same flow channels and power consumption, the temperature of liquid cooling BTM module is lower, ensuring better temperature uniformity.[28] The direct cooling of battery packs using refrigerants has emerged as a new cooling solution in recent years. Through experiments conducted under vehicle conditions, a comparison is made between the thermal performances of two-phase refrigerant cooling and liquid cooling with the same outer diameter. Even under harsh environmental conditions, the 45 °C maximum temperature of the battery can be met by refrigerant cooling.[29] When the cooling mode changes from refrigerant cooling to liquid cooling under 2C charging, the heat transfer coefficient reduces about 73.6%, and the battery temperature increases by about 12 °C.[30] So, refrigerant cooling is considered the preferred alternative to traditional liquid cooling.[31] Its reliable performance, coupled with a simple structure and lightweight design, makes it an attractive option. Especially in plug-in hybrid series, where both an engine and a battery module coexist, the compact layout demands efficient space utilization. Refrigerant cooling methods offer a simpler structure, space-saving attributes, and reduced costs, which explains their widespread adoption in plug-in hybrid series. Table 1 lists the advantages and disadvantages of mainstream BTM.[32]

The air conditioning (AC) of EVs uses an electric compressor driven by electric energy to generate the cold capacity. The common BTM is shown in Figure 1. As the only fluid in the BTMS of refrigerant cooling, the refrigerant plays an irreplaceable role in the cooling system. Direct refrigerant cooling involves flowing the refrigerant directly into the battery


https://doi.org/10.1021/acsomega.4c02902
ACS Omega 2024, 9, 25591−25609

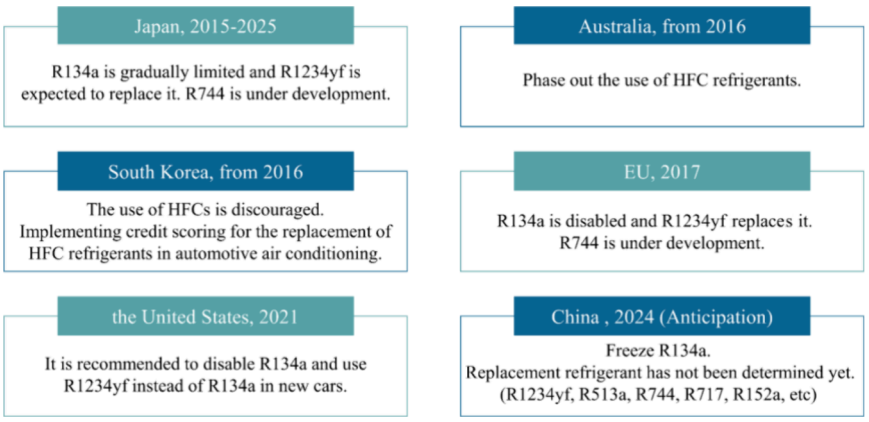



**Figure 2.** Refrigerant replacement program.

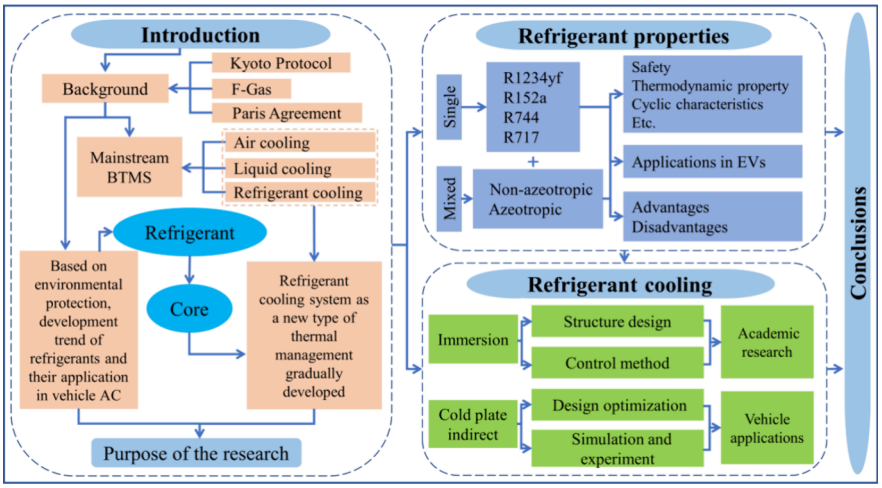



**Figure 3.** Technical route schematic diagram.

module (pipe or vessel). Refrigerant cooling involves the direct flow of refrigerant into the battery pack.[15] The low-temperature, low-pressure refrigerant is compressed by the compressor into a high-temperature, high-pressure gas. Through the condenser, it exchanges heat with the surrounding environment, cooling, and condensing into a high-pressure liquid state. The liquid refrigerant then passes through a throttling device, rapidly depressurizing and expanding, thereby reducing the temperature and pressure. Ultimately, the low-pressure two-phase refrigerant, in the evaporator, absorbs heat and transforms into a low-temperature,[33] low-pressure gas.[34] This process involves the refrigerant evaporating inside the battery pack, directly dissipating the battery heat. Compared with liquid cooling, its advantage lies in reducing intermediate heat transfer processes, such as the heat exchanger shown in Figure 1(b), enhancing energy efficiency, and reducing additional components such as liquid coolant pipelines and water pumps, further lowering costs. Refrigerant, as the cooling medium of the vehicle AC system, is an essential auxiliary system for BTM. However, the extensive use of AC also brings another environmental problem: the greenhouse effect.[35,36]

Traditional refrigerants may damage the atmospheric ozone layer and cause environmental pollution. There is a shift toward using green and environmentally friendly refrigerants to protect the environment.[37] Since 1997, a series of international agreements such as Kyoto Protocol,[38] F- Gas,[39] and Paris Agreement[40] have been successively implemented, gradually elevating the issues of greenhouse gas emissions and environmental conservation onto the agenda. This agreement emphasized that the reduction of refrigerant emissions is one of the key measures.[41]

Various measures have been taken by countries around the world to reduce refrigerant emissions. While some nations have encouraged the use of ecologically benign refrigerants, others have imposed limitations and prohibitions on the use of refrigerants. In addition, researchers are also developing new refrigeration technologies to reduce the refrigerants used or to completely replace them.[42] The timeline and alternative refrigerants for the use of high global warming potential (GWP) refrigerants in vehicle AC systems in several major automobile countries globally are shown in Figure 2.

Existing reviews and studies mostly focus on liquid cooling and PCM cooling, with relatively few studies on BTMS of refrigerant cooling. In addition, R134a is commonly used as the charging refrigerant in BTMS, but its GWP is around 1430. Given the current situation, it is necessary to find suitable alternatives. Therefore, this paper offers a systematic review of the recent applications and advancements in research of refrigerants in vehicle AC systems and refrigerant cooling in BTM. Emphasis is placed on summarizing pertinent experimental and simulation studies from two perspectives: immersion and cold plate indirect cooling, analyzing the application of refrigerants, and the current progress and future


https://doi.org/10.1021/acsomega.4c02902
ACS Omega 2024, 9, 25591−25609

development trends of refrigerant cooling technology. It is hoped that this paper can expand the understanding of BTM among researchers and readers and play a constructive role in the advancement of relevant domains. The technical route is shown in Figure 3.

## 2. CURRENT STATUS AND RESEARCH PROGRESS OF REFRIGERANTS

Refrigerants are the core components used for cooling in refrigeration systems. Different refrigerants possess distinct physicochemical properties that may impact the effectiveness of the AC system. Commonly used refrigerants include single refrigerants and mixed refrigerants. This section presents a systematic review on the types, properties, and advantages and disadvantages of alternative refrigerants. The research on the application of replacement refrigerant in vehicle AC can provide a useful reference for the BTM of refrigerant cooling.

**2.1. Single Refrigerants.** Single refrigerants refer to a single substance used as a refrigerant, typically a low-boiling gas or liquid. Single refrigerants are usually compressed into a liquid state and then released through an expansion valve or throttle device in the refrigeration equipment, carrying heat away from the refrigeration system to accomplish the objective of temperature reduction. The most commonly used single refrigerants currently include R134a, R22, R32, etc.[43,44]

Table 2 lists the commonly used single refrigerants.[45,46] CFCs have been banned by most countries due to their nonzero ozone depletion potential (ODP), potential risks to the ozone layer, and high GWP. In contrast, HFOs are gradually becoming popular as substitutes. Additionally, R744 ($CO_2$) is also considered a promising single refrigerant, although its low-temperature performance still needs to be further improved.[47]

**Table 2. Classification of Single Refrigerant**

| Classification | Example |
|---|---|
| Chlorofluorocarbons (CFCs) | R11, R12, R13 |
| Hydrochlorofluorocarbons (HCFCs) | R22, R123 |
| Hydrochlorofluoroolefins (HCFOs) | R1233zd(E) |
| Hydrofluorocarbons (HFCs) | R23, R32, R134a, R152a |
| Hydrofluoroolefins (HFOs) | R1234yf, R1234ze(E) |
| Hydrocarbons (HCs) | R290 (Propane), R600 (Butane) |
| Perfluorocarbons (PFCs) | R116, R218 |
| Others | R744 ($CO_2$), R717 ($NH_3$), RE170 (Dimethyl ether) |

*2.1.1. Environmental Impact and Safety of Single Refrigerants.* Currently used single refrigerants can also have certain environmental impacts during production and use.[48] Although their ODP is zero and does not cause damage to the atmospheric ozone layer like CFCs, HCFCs, and HCFOs, they still have a certain residence time in the atmosphere and have an impact on global warming and the greenhouse effect.[49] In addition, the preparation and recovery of single refrigerants also generate some carbon emissions and energy consumption. Controlling their usage and reducing leakage are necessary steps to lessen the environmental impact that single refrigerants produce.[50] Furthermore, it is necessary to increase research on the recovery and reuse of individual refrigerants to reduce energy consumption and emissions during the preparation and recovery process.

Single refrigerants also have certain safety risks in their use processes, such as flammability, explosiveness, and toxicity. For example, R32 is flammable and explosive at high concentrations, R290 is highly flammable and explosive, and R717 is highly toxic. Therefore, safety issues should be considered in the design and use of refrigeration systems to ensure the safety of personnel and equipment.[51] Table 3 lists some of the thermal properties of commonly used refrigerants.

According to ASHRAE standard, refrigerant is divided into three toxicity grades: A (nontoxic), B (weak toxic), and C (toxic). At the same time, according to the lower explosion limit (LEL), the refrigerant can be divided into four combustion grades: 1 (nonflammable), 2L (light combustible), 2 (combustible), and 3 (inflammable).

*2.1.2. Application of Single Refrigerants in EVs.* The predominant refrigerant utilized in current vehicle AC systems is R134a. However, due to its high GWP, R134a contributes to the greenhouse effect. To meet increasingly stringent environmental requirements, green and environmentally friendly refrigerants are needed. As a result, research has shifted toward low-GWP single refrigerants, such as R744 ($CO_2$), R717 ($NH_3$), R1234fy, and R152a. Compared with CFCs, these single refrigerants have advantages such as environmental friendliness, high efficiency, and safety, which align with the development direction of NEVs.

R744 ($CO_2$) is a natural refrigerant[52] that is a colorless, odorless, nontoxic, nonflammable, and nonexplosive single refrigerant with the advantages of being ecologically beneficial, efficient, and safe. Due to its short atmospheric lifetime, $CO_2$ does not destroy the ozone layer, and is thus known as a "green refrigerant".[53] R744 has superior thermodynamic properties, resulting in a higher refrigeration efficiency and lower greenhouse gas emissions. As a result, it has broad applications in the area of NEVs.

**Table 3. Thermal Properties of Single Refrigerants**

| refrigerants | molecular weight (g/mol) | boiling point (°C) | critical temperature (°C) | GWP | ODP | safety classification |
|---|---|---|---|---|---|---|
| R12 | 120.91 | −29.8 | 111.97 | 10800 | 1 | A1 |
| R22 | 86.47 | −40.8 | 96.15 | 1760 | 0.055 | A1 |
| R32 | 52.02 | −51.7 | 78.11 | 677 | 0 | A2L |
| R134a | 102.03 | −26.1 | 101.06 | 1430 | 0 | A1 |
| R152a | 66.05 | −24.0 | 113.26 | 138 | 0 | A2 |
| R1234yf | 114.04 | −29.5 | 94.70 | 4 | 0 | A2L |
| R290 | 44.10 | −42.1 | 96.74 | 5 | 0 | A3 |
| R744 | 44.01 | −78.5 | 30.98 | 1 | 0 | A1 |
| R717 | 17.03 | −33.3 | 132.25 | 0 | 0 | B2L |



https://doi.org/10.1021/acsomega.4c02902
ACS Omega 2024, 9, 25591−25609

Researchers[53,54] conducted a comparative analysis of the performance for heat pumps (HPs) using R744 and R134a in EVs. At a certain heating capacity, the coefficient of performance (COP) of the R744 unit is 51% higher than the R134a unit. Song et al.[55] analyzed the feasibility of a transcritical R744 vehicle AC system for electric buses under different environmental conditions. Results indicate a decrease in COP and refrigeration capacity by 35% and 27.4%, respectively, when the ambient temperature rises from 35 to 45 °C. The energy efficiency of R744 increases with higher indoor temperatures.

However, because of its high working pressure and temperature, the system design and manufacturing requirements for $CO_2$ are relatively complex and demanding. Compared with other conventional refrigerants, $CO_2$ has higher manufacturing and usage costs, which limit its development. Researchers find that R744 has a significantly greater unit cooling capacity per unit volume than R134a and has excellent thermal conductivity. The use of R744 in vehicle AC systems has significant advantages, but there are also some drawbacks. For example, R744 requires a transcritical cycle, which results in much higher operating pressures than R134a, resulting in high compressor discharge temperatures, and requires modifications to existing pipelines before it can be used.[47,56] Likewise, within the BTMS, modifications are necessary to pressurize the evaporator pipelines within the battery module to accommodate the high evaporation pressure associated with the R744.

R717 is a colorless and pungent natural refrigerant with excellent thermodynamic properties and refrigeration performance, widely used in industrial refrigeration and AC systems.[57] It naturally degrades in the atmosphere and does not pose a threat to the ozone layer with relatively little impact on the environment. Moreover, it has high latent heat of evaporation and fluidity, making it easy to diffuse in the event of leakage and reducing the risk of explosion and fire. Compared with traditional compounds, R717 has higher refrigeration efficiency and environmental friendliness, making it an attractive choice for widespread applications.[58] However, some drawbacks need to be noted: R717 has high corrosiveness and requires high-quality materials for pipes and valves for refrigeration systems. Furthermore, R717 is a toxic gas that is harmful to human health; therefore, safety measures must be taken during use and transportation.

R152a is a colorless and odorless monomeric refrigerant with good refrigeration and environmental performance. Compared with R134a, R152a has a lower greenhouse effect and higher refrigeration efficiency.[59] However, R152a is susceptible to contamination by impurities, such as moisture and oxides, and its stability is inferior to that of other refrigerants. Due to its combustibility, strict control is necessary to ensure safe use, resulting in restrictions on its application under certain special conditions.[60] The use of the R152a refrigerant in EVs has already been studied. Research studies have shown that R152a has a higher refrigeration capacity and COP compared with R134a. Mixing R152a with other refrigerants can improve its stability, making it a more promising low-GWP substitute.[61,62] In addition, there are studies that have improved the efficiency and safety of AC systems through design improvements.[63] Overall, although the application of R152a refrigerant in EVs still faces certain challenges, its advantages in energy efficiency and environmental protection are still worth exploring and researching further.[64]

Direk et al.[65] found that, based on the optimal COP, the optimal charge amounts for R152a and R134a are 625g and 512g, respectively. Compared with R134a, R152a has the highest cooling capacity. On the other hand, the R152a has the highest COP value at all compressor speeds. Serevina et al.[66] found that while R152a has higher discharge temperatures, it exhibits a 6.4% higher COP compared with R134a, a difference that diminishes under no-load conditions.[67] Several scholars[68,69] also research the performance of R134a and R152a, yielding similar outcomes. Sumeru et al.[70] estimated the operational efficiency of R152a vehicle AC systems at various compressor speeds and condensing temperatures. At 50 °C, R152a demonstrates an approximately 5% higher refrigeration capacity than R134a. The impact of condensing temperature on the COP of R152a outweighs that of compressor speed. Ma et al.[71] found that, as the gas engine heat pump speed increased from 1200 to 1600 rpm, the isentropic efficiency and volumetric efficiency of using R152a increased by 3.5−10.7% and 5.8−7.3%, respectively, compared with R134a. The results show that the use of R152a has a higher heating efficiency and compressor efficiency.

R1234yf is a new type of single refrigerant that is nonflammable and nontoxic. It is one of the alternative refrigerants that can substitute for R134a.[72] At present, scholars from various countries have studied its physical properties and heat transfer characteristics through experimental methods. The molecular formula of R1234yf is $CF_3CF{=}CH_2$, its ODP is zero, its GWP is 4, and its atmospheric lifetime is 11 days. It has excellent environmental friendliness.[73,74] More and more cars are starting to use R1234yf in AC systems. Compared with R134a, the theoretical cycle performance of the two is very close, and the operating pressure is almost the same. R1234yf can be filled and used in existing systems without changing their structure. Studies[75,76] have shown that, with an extended vehicle testing time, R1234yf exhibits a faster cooling ability than R134a, and the temperature decrease trend is very similar, approaching consistency. However, the substitution of R134a with R1234yf leads to a 25% reduction in the system cooling efficiency.[77] Zhao et al.[78,79] compared the performance of vehicle AC systems using R1234yf and R134a under different working conditions. These tests encompass different thermal loads, compressor speeds, condenser and evaporator fan speeds, and environmental and indoor conditions (temperature and relative humidity). The optimal charge amounts for R134a and R1234yf are found to be 1000g and 950g, respectively. Test results indicate that under all conditions, the COP and refrigeration capacity of the R134a system outperform those of the R1234yf system by 12.4% and 9%, respectively. But the cost of R1234yf is higher than that of traditional refrigerants, and it is protected by patents, so the cost of AC systems using R1234yf would also be higher (the R1234yf cost is 20 times that of the R134a refrigerant cost). In European and North American countries and regions, R1234yf has begun to be gradually adopted for use in new vehicles.

Compared with those of R134a, the advantages and disadvantages of common single refrigerants are shown in Table 4.

In summary, single refrigerants have the advantages of being environmentally friendly, energy-efficient, and safe, making them widely applicable in the field of NEVs. However, due to


https://doi.org/10.1021/acsomega.4c02902
ACS Omega 2024, 9, 25591−25609

Table 4. Advantages and Disadvantages of Single Refrigerants

| refrigerants | advantages | disadvantages |
|---|---|---|
| R744 | Low-GWP | Transcritical |
| | Greater unit cooling capacity per unit volume | High working pressure |
| R717 | Excellent refrigeration performance | Strong causticity |
| | High latent heat | Toxic |
| R152a | Low-GWP | Combustible |
| | Excellent refrigeration efficiency | Low stability |

the significant differences in boiling point, density, and thermodynamic properties among single refrigerants, it is necessary to select appropriate refrigerants based on different application scenarios. Furthermore, it is essential to strengthen the exploration of single refrigerants, explore more environmentally friendly, efficient, and safe refrigerants, and actively promote their application in the field of NEVs.

**2.2. Mixed Refrigerants.** Mixed refrigerants consist of two or more different substances. The properties and characteristics of mixed refrigerants are determined by the properties and characteristics of the refrigerants that make up the mixture. Different combinations of refrigerants can result in different refrigeration performances, which a have higher refrigeration efficiency and a wider range of applications. It has advantages that single refrigerants cannot achieve. Compared with single refrigerants, mixed refrigerants have wider operating temperature ranges, higher refrigeration efficiencies, and less environmental pollution.[80] Common mixed refrigerants include R32/R125, R134a/R152a, R134a/R1234yf, etc.[81,82] Some scholars have also proposed multicomponent mixed refrigerants as alternatives to existing single refrigerants based on thermodynamic properties, cycle performance, safety, and other aspects.[83,84]

According to the characteristics of mixed refrigerants, they can be categorized into two distinct types: non-azeotropic mixed refrigerants and azeotropic mixed refrigerants. This section provides a detailed introduction to the properties, applications, advantages, and disadvantages of these two types of mixed refrigerants.

*2.2.1. Non-Azeotropic Mixed Refrigerants.* Non-azeotropic mixed refrigerants[85] are refrigerants composed of two or more substances that do not meet the condition of a coexisting saturated vapor and saturated liquid. The boiling point of the mixture changes with the proportion of its components, and therefore, it is also referred to as an "incompatible mixture".[86] The components of non-azeotropic mixed refrigerants undergo phase separation into a vapor and liquid at a constant temperature, which affects various components in the refrigeration cycle.

The stability of non-azeotropic mixed refrigerants depends on their composition and temperature. An increase in temperature can cause component separation and uneven mixing, which, in turn, can affect the refrigeration performance and system stability. The physical properties of the mixture also vary with the proportion of each substance present in the mixture.[87] Therefore, when non-azeotropic mixed refrigerants are used, it is important to pay attention to their composition and usage conditions to ensure their proper use and safe operation.

The condensation and vaporization temperatures of non-azeotropic mixed refrigerants vary with the composition of the mixture, a phenomenon known as the temperature glide effect. In the heat transfer process, the temperature glide effect affects the temperature distribution and thermal conductivity of each component in the mixture, thereby affecting the efficiency of heat transfer. At a constant temperature, the components of non-azeotropic mixed refrigerants undergo phase separation into vapor and liquid.[88] This phenomenon can cause overheating or overcooling problems in components such as compressors, evaporators, and condensers in refrigeration systems. Meng et al.[89] introduced a mixture of R1234yf and R134a (89:11) applied in a vehicle AC system. The vehicle AC system using this mixture exhibits a 16% lower COP in HP mode and a 9% lower COP in AC mode compared with that of R134a. It is noteworthy that flammability issues are avoided when R134a (mass ratio of 11%) is included. Scholars[90,91] use R134a mass ratios of 5%, 10%, and 15% in R1234yf.

In practical applications, non-azeotropic mixed refrigerants are commonly used in low-temperature refrigeration and AC systems. Due to their special properties, refrigeration systems that use non-azeotropic mixed refrigerants require higher safety standards and stricter operating requirements. Therefore, when non-azeotropic mixed refrigerants are chosen, it is necessary to carefully assess their risks and safety.

*2.2.2. Azeotropic Mixed Refrigerants.* Azeotropic refrigerants are composed of two or more refrigerants mixed in a certain proportion and have a common boiling point. In the process of the vapor phase or liquid phase under constant pressure, the composition of the vapor and the composition of the solution remain unchanged, and the corresponding temperature remains constant.[92] Changes in the component content may cause changes in the boiling point and dew point (the temperature at which saturated vapor and liquid are in equilibrium) of the azeotropic mixture. Therefore, the component contents of the mixture must be precisely controlled. In azeotropic mixtures, there are interactions between different components, which affect the transport properties of each component in the mixture, including heat and mass transfer.[92,93] The thermodynamic properties of azeotrope refrigerant are different from those of a single substance before mixing, and the characteristics of the refrigerant can be improved by mixing, providing greater freedom for modulating the properties of the refrigerant and expanding the selection of the refrigerant. For example, azeotropic refrigerants may maintain a stable evaporation temperature at a certain pressure, which is very advantageous for refrigeration systems that require precise temperature control.

Azeotropic mixed refrigerants have many advantages. First, the boiling point of the mixtures is constant, so refrigeration systems using azeotrope mixtures can be more stable and reliable.[93] Second, azeotropic mixed refrigerant has a low gasification pressure, which can reduce the working pressure of the system, resulting in reduced energy consumption and system costs.[94] In addition, the azeotrope mixed refrigerant has good stability, is not easy to decompose or stratify, and is easy to prepare and operate. The special properties of azeotrope can also alleviate the environmental problems and use restrictions of a single refrigerant to some extent.

There is a nonlinear relationship between the temperature and pressure of azeotrope mixtures called the temperature−pressure mole fraction curve. The shape and position of this curve depend on the constituent components of the mixture. The mixed properties of azeotropic refrigerant mixtures are


https://doi.org/10.1021/acsomega.4c02902
ACS Omega 2024, 9, 25591−25609

more complex than single refrigerants and require more advanced thermodynamic calculations.[95]

Azeotropic mixtures exhibit excellent thermodynamic properties.[96] These mixtures can simultaneously boil and condense, enabling refrigeration systems to operate over a wider range of temperatures and pressures. Besides, azeotropic mixtures possess high latent heat of condensation and evaporation, which implies that under the same working conditions they can provide a higher cooling capacity. The composition of the azeotropic mixtures is stable and can remain stable at different temperatures and pressures. Therefore, in refrigeration or AC systems, there will be no component separation, making the system operate more stably and reliably.[97]

Mixed refrigerants are widely used, and different proportions of single refrigerants can form mixed refrigerants with different properties, providing a broader space for exploration and research.

## 3. REFRIGERANT COOLING

Refrigerant cooling refers to the process of using refrigerants to cool batteries. This is done by utilizing the cooling properties of the refrigerants to lower the batteries temperature. According to the contact mode between the refrigerant and the battery, it can be divided into immersion cooling (that is, direct cooling) and indirect cooling through a cold plate.

**3.1. Immersion Cooling.** Immersion cooling is an efficient method for managing the battery temperature. Schematic diagram of immersion cooling is shown in Figure 4. This

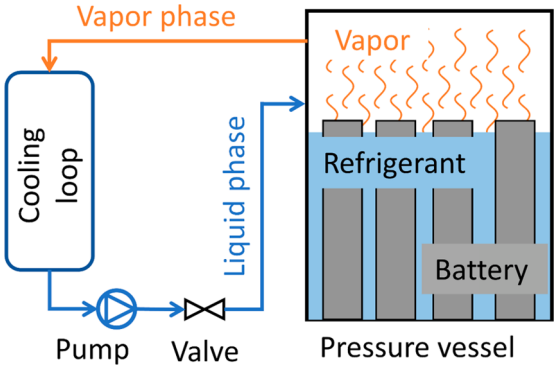



**Figure 4.** Schematic diagram of immersion cooling (two-phase).

method immerses the battery in a refrigerant (or coolant) to directly cool it, which has a higher heat transfer efficiency and facilitates rapid heat transfer from the battery to the refrigerant, resulting in more effective temperature control. Compared with common liquid coolants, refrigerant immersion cooling (including certain electronic fluorinated fluids like Novec-649,[97] Novec-7000,[98] HFE-7100,[99] etc.) primarily utilizes the latent heat of vaporization released during the phase change of the refrigerant from liquid to vapor to absorb heat from the battery, known as boiling cooling. Conversely, single-phase liquid immersion cooling (such as hydrocarbons, esters, silicone oils, and water-based fluids) absorbs heat from the battery using the sensible heat of dielectric fluids. Typically, due to the lower boiling points of refrigerants in AC systems, using refrigerants as working media in immersion cooling studies requires the utilization of a pressure vessel. Immersion cooling possesses a distinct advantage in achieving thermal homogenization of battery by controlling the boiling point temperature of refrigerant, thereby enabling more uniform cooling of the battery and reducing the temperature gradient.[100] This cooling method has the advantages of good refrigeration effect and temperature stability but faces technical challenges such as the stability of the immersed liquid and the sealing of the battery casing. Currently, research on immersed cooling for managing the temperature of power batteries is still in its early or nascent stages.[101−105]

In experimental and simulation processes, the heat generation of the battery adopts eq 1:[34,69]

$$P = \frac{dQ_b}{dt} = I\left[(E_0 - U) - T\frac{dE_0}{dT}\right] = \left[I^2R_i - T\frac{dE_0}{dT}\right] \quad (1)$$

where $P$ represents heat generation power, $Q_b$ denotes battery heat generated, $I$ is battery current, $E_0$ stands for operating voltage, $U$ is open-circuit voltage, $T$ represents temperature, and $R_i$ is internal resistance. The relationship between the internal resistance and state of charge (SOC) is obtained using linear regression fitting. The volume heat generation rate $q_b$ is calculated as follows:

$$q_b = \frac{P}{V_b} \quad (2)$$

where $V_b$ represents the volume.

The thermal behavior of the battery and the heat distribution of the refrigerant in the vapor phase can be found by three-dimensional heat transfer and mass flow models.[102,103]

$$\nabla\cdot\left(k_b\left(\frac{\partial T_b}{\partial x}i + \frac{\partial T_b}{\partial y}j + \frac{\partial T_b}{\partial z}k\right)\right) + q_b - q_c = \left(\frac{\partial \rho_b}{\partial t}\cdot\frac{\partial c_{p,b}}{\partial t}\cdot\frac{\partial T_b}{\partial t}\right) \quad (3)$$

where, $k_b$, $T_b$, $\rho_b$, and $c_{p,b}$ indicate the thermal conductivity, temperature, density, and specific heat capacity of the battery, respectively, and $q_c$ is the volume heat dissipation rate.

This section describes the current state and research progress of the refrigerant immersion cooling in BTM of EV, including the structural design and control strategy of immersion cooling.[102,103] Moreover, the issues and future research directions of immersion cooling will be discussed. First, the basic structural design of a battery immersed in refrigerant will be introduced. Second, the influence of refrigerant on battery temperature and optimization of control strategies will be analyzed.[104] Finally, the future development direction of refrigerant immersion cooling for batteries will be explored.

*3.1.1. Structure Design.* The structural design of the immersion cooling of batteries in refrigerant includes factors such as the depth of refrigerant immersion, direction, and speed of refrigerant flow, and the size matching of batteries and cooling systems. A reasonable design of these factors can improve cooling efficiency and reduce the system pressure drop, as well as minimize refrigerant usage and energy consumption. The basic structure of battery immersion cooling in refrigerant is shown in Figure 5.

Zhao et al.[106] compared the highest temperature, temperature difference (TD), and capacity decay of lithium-ion batteries under three cooling conditions (direct evaporation cooling, air cooling, and free convection cooling). The


https://doi.org/10.1021/acsomega.4c02902
ACS Omega 2024, 9, 25591−25609

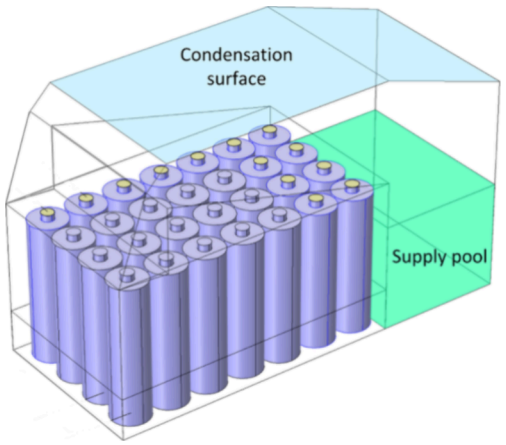



**Figure 5.** Basic structure of battery immersion cooling in refrigerant.[103] Reprinted with permission from ref 103. Copyright 2020 Elsevier.

experimental findings illustrate that the proposed direct evaporation cooling (immersion cooling) system has the capability to broaden the operational boundaries of lithium-ion batteries, enabling their application in increasingly rigorous and demanding working environments. Scholars also explore pool boiling heat management schemes based on R290,[107] R717,[108] and R134a.[109] The results indicate that as the saturation vapor pressure of the refrigerant increases, the temperature uniformity of the battery module is significantly enhanced. However, it is crucial to note that this can also result in a notable increase in the battery temperature. Among them, the selection and arrangement of battery modules are important factors affecting the effectiveness of the battery immersion cooling technology in refrigerants. The selection of battery modules should consider factors such as their volume, shape, and heat dissipation. The liquid height of the refrigerant is another crucial aspect. Al-Zareer et al.[110] showed that the spacing between batteries immersed in R134a can be ignored. The compact structure of the system allows for the immersion of the battery in the refrigerant, resulting in the maximum temperature of 35 °C and a temperature variation of no more than 4 °C when the immersion ratio is at 80%. Goodarzi et al.[111] discovered through experimental research that raising the immersion height of the refrigerant (R-141b) and decreasing the pressure yielded a decrease in the maximum temperature of the battery pack. The batteries are operated at 4C, and under immersion conditions of 25%, 50%, 75%, and 100%, the maximum temperatures are reduced by 18.4 °C, 24.3 °C, 27.1 °C, and 30.7 °C, respectively, compared with the noncooled condition. Additionally, increasing the refrigerant height also reduces the TD between batteries and within each individual battery.

*3.1.2. Control Method.* In the study,[105] the experimental investigation focuses on the immersed-phase change cooling performances of R1233ZD(E)/ethanol mixture. Coupled boiling heat transfer and forced convection analysis are conducted on the staggered battery module under different discharge rates, R1233ZD(E) filling volume fractions, and inlet flow rates, as shown in Figure 6. The research results indicate that when R1233ZD(E) is combined with ethanol, it effectively enhances the boiling heat transfer on the wall, leading to an obvious improvement in the temperature uniformity of the battery module by 57.0%.

In addition, the researchers[104] propose another immersion cooling scheme based on HFE-7000, as shown in Figure 7. The results indicate that nucleate boiling is more effective in controlling the TD of batteries. Compared with conventional liquid cooling strategies, the immersion cooling system based on HFE-7000 can limit the maximum TD during a 3C discharge rate to within 4.3 °C. In the pool boiling TMS that was previously detailed, visible bubbles emerge on the battery wall when the overheating exceeds 5.0 °C. Otherwise, free convection in the liquid phase predominantly influences the heat transfer process. A study[98] proposes a boiling-cooling TMS based on HFE-7000 refrigerant, as shown in Figure 8, an approach which proves effective in reducing the maximum temperature and TD of large-size lithium-ion batteries. Through experiments in three different modes: static, flow, and intermittent flow, it is ultimately demonstrated that the boiling-cooling system employing an intermittent flow strategy

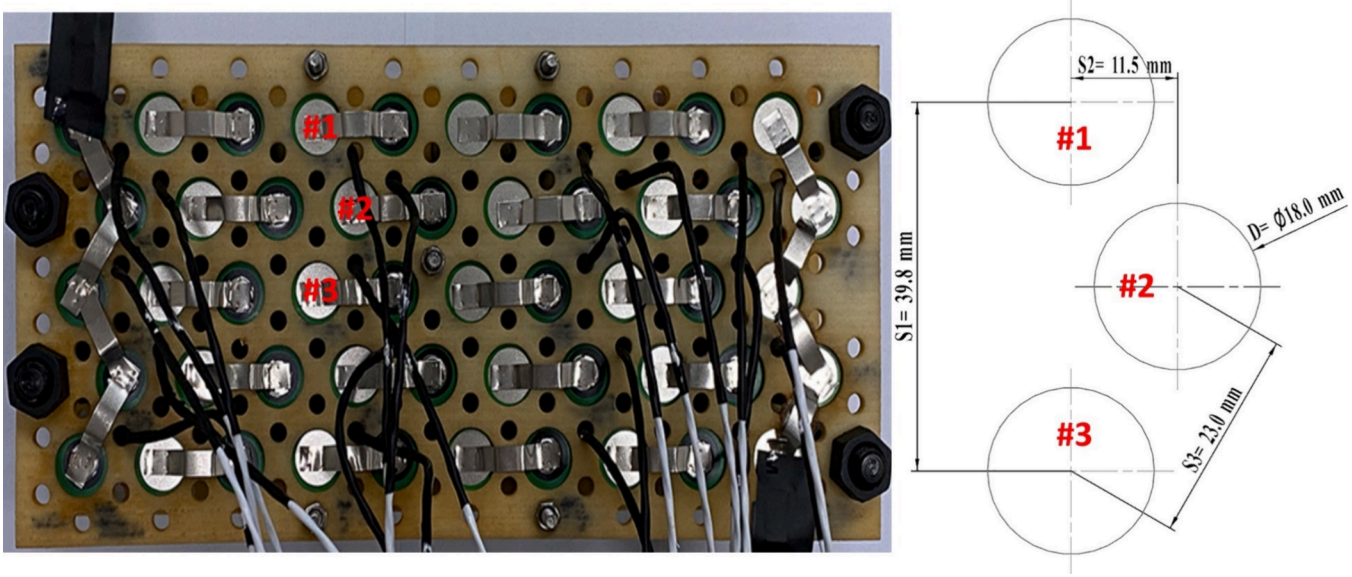



**Figure 6.** Staggered battery layout.[105] Photograph courtesy of Wang et al. Reprinted with permission from ref 105. Copyright 2023 Elsevier.


https://doi.org/10.1021/acsomega.4c02902
ACS Omega 2024, 9, 25591−25609

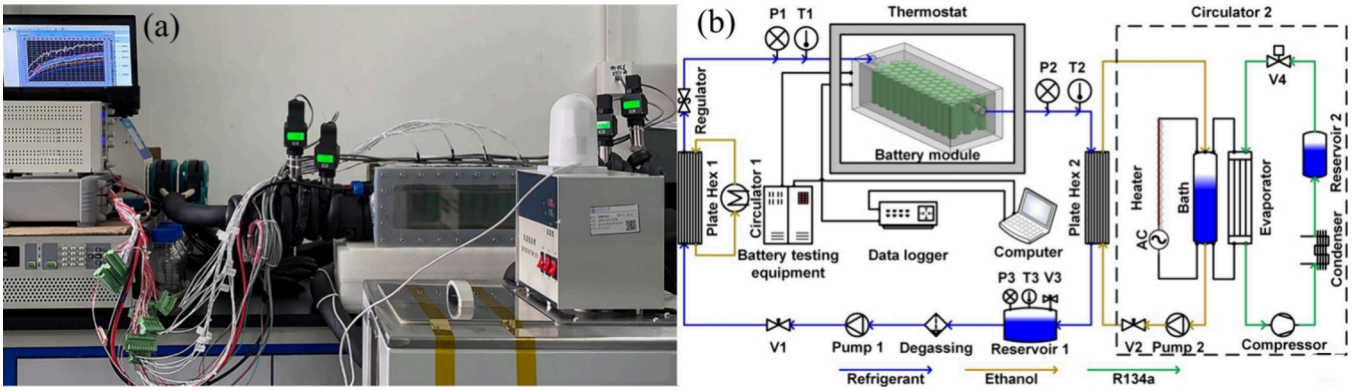



**Figure 7.** Battery immersion cooling:[104] (a) Experimental equipment. (b) Schematic diagram. Photograph courtesy of Wang et al. Reprinted with permission from ref 104. Copyright 2020 Elsevier.

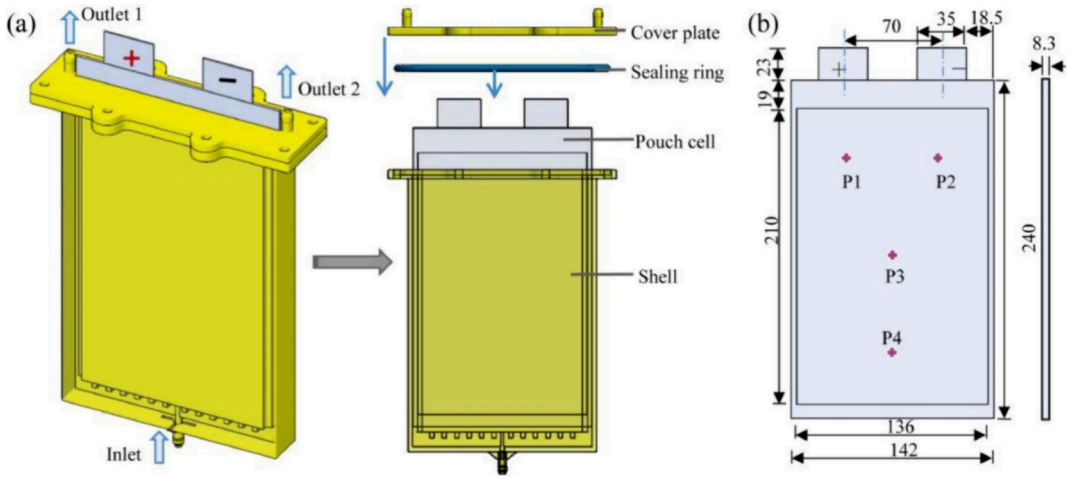



**Figure 8.** Schematic representation of the test specimen:[98] (a) Cooling structure. (b) Structure size and monitoring site distribution. Reprinted with permission from ref 98. Copyright 2021 Elsevier.

**Table 5. Immersion Cooling Main Research Content Summary**

| sources | battery | working condition | refrigerant | focus | results | method |
|---|---|---|---|---|---|---|
| 98 | $LiFePO_4$ 20 Ah | 1C−4C | Novec 7000 | Boiling cooling system with intermittent flow mode | In 4C discharge rate, the surface temperature of the battery is controlled below 36 °C, and the temperature uniformity is greatly improved. | Experiment |
| 104 | NCM 811 3.2 Ah 3.6 V | 5C | HFE-7000 | HFE-7000 flows and boils on the battery wall surfaces. | Inlet is 0.3 m/s and 5C discharge rate; the maximum temperature is reduced to 35.10 °C. | Experiment/ Simulation |
| 105 | NCA 2.6 Ah 3.6 V | 1C−3C | R1233ZD(E)/ Ethanol | Different discharge rates, filling volume fractions, and inlet volume flow rates | When R1233ZD(E) is mixed with ethanol, the wall boiling heat transfer is enhanced, and the temperature uniformity is increased by 57.0%. | Experiment |
| 109, 110 | Sony 18650 | 5C | R134a | Liquid phase R134a partial immersion battery module | Refrigerant-based immersion cooling has excellent performance. | Simulation |
| | | 6C−8C | | | | |
| 111 | 18650 2.6 Ah 3.6 V | 4C | R-141b | Refrigerant height, ambient temperature, and vessel pressure | Under the condition of 100% immersion and 4C discharge rate, the maximum temperature drops from 71.2 to 40.5 °C. | Experiment |

can achieve efficient thermal management. Table 5 summarizes the main research contents of immersion cooling.

**3.2. Cold Plate Indirect Cooling.** Cold plate indirect cooling belongs to refrigerant flow boiling cooling,[112,113] which is another cooling method for BTMS. It refers to reducing the battery temperature by passing the refrigerant through the heat sink on the outside of the battery module. Convective heat transfer and bubble boiling heat transfer take place within the mini-/microchannels of the cold plate[114] and not in direct contact with the battery wall. By using the refrigerant as the heat transfer medium, the battery heat is transferred to the cold plate, thereby achieving the purpose of heat dissipation.

The main components of this method include battery modules and a refrigerant circulation system. The batteries are the source of heat generation, while the refrigerant circulation system is the medium that removes heat from the battery. The refrigerant circulation system typically consists of a compressor, condenser, throttle device, and evaporator. Its working principle is to convert the refrigerant into a liquid or gas state under different pressures, thereby removing heat from the


https://doi.org/10.1021/acsomega.4c02902
ACS Omega 2024, 9, 25591−25609

battery. Here, the cold plate acts as the evaporator,[115] where the low-temperature and low-pressure refrigerant directly enters the cold plate for heat exchange with the battery module. The cold plate indirect cooling system replaces the evaporator in AC systems and the chiller in liquid cooling systems,[64] as shown in Figures 9 and 10. This eliminates the liquid system in traditional liquid cooling systems. Compared with traditional liquid cooling systems, this direct cooling system has a smaller volume, occupies less space, avoids the risk of liquid leakage in liquid cooling systems, and has a higher cooling efficiency. This section will introduce the current situation and research progress of cold plate indirect cooling technology in the BTM of EV.

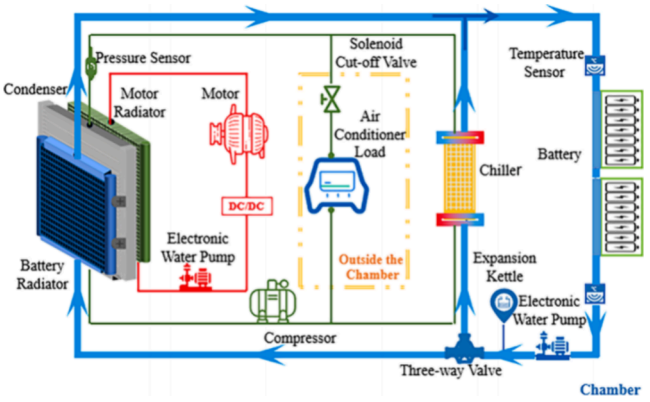



**Figure 9.** Schematic diagram of liquid cooling.[64] Reprinted with permission from ref 64. Copyright 2022 Elsevier.

The cold plate indirect cooling based on refrigerant has advantages such as a stable refrigeration effect and no impact on battery sealing, but its refrigeration efficiency is relatively lower than that of the immersion cooling. A key component of the cooling technology is the cold plate, which is responsible for removing the heat generated on the battery surface.[13] The cold plate needs to have characteristics such as high mechanical strength, corrosion resistance, high temperature resistance, and high thermal conductivity.[26] Currently, common cold plate materials include aluminum alloys, copper alloys, and composite materials. Among them, aluminum is often used as cold plate material due to its high thermal conductivity and suitable cost.

Research on cold plate indirect cooling based on refrigerant technology for BTM of EV has been continuously deepened and developing. Currently, domestic and international researchers have extensively researched and explored the optimization and integration of cold plate indirect cooling technology.[116] The research on optimization methods mainly includes refrigerant flow optimization, cold plate layout optimization, and temperature control optimization. By researching the optimization methods of cold plate indirect cooling technology, scholars have continuously improved its thermal management effectiveness and operational stability.

In the two-phase medium, the problem of two-phase flow and heat transfer is solved by eqs 4−14.[103,115,117]

Continuity equations:

$$\frac{\partial \rho_m}{\partial t} + \nabla \cdot (\rho_m \overline{v}_m) = \overline{m} \tag{4}$$

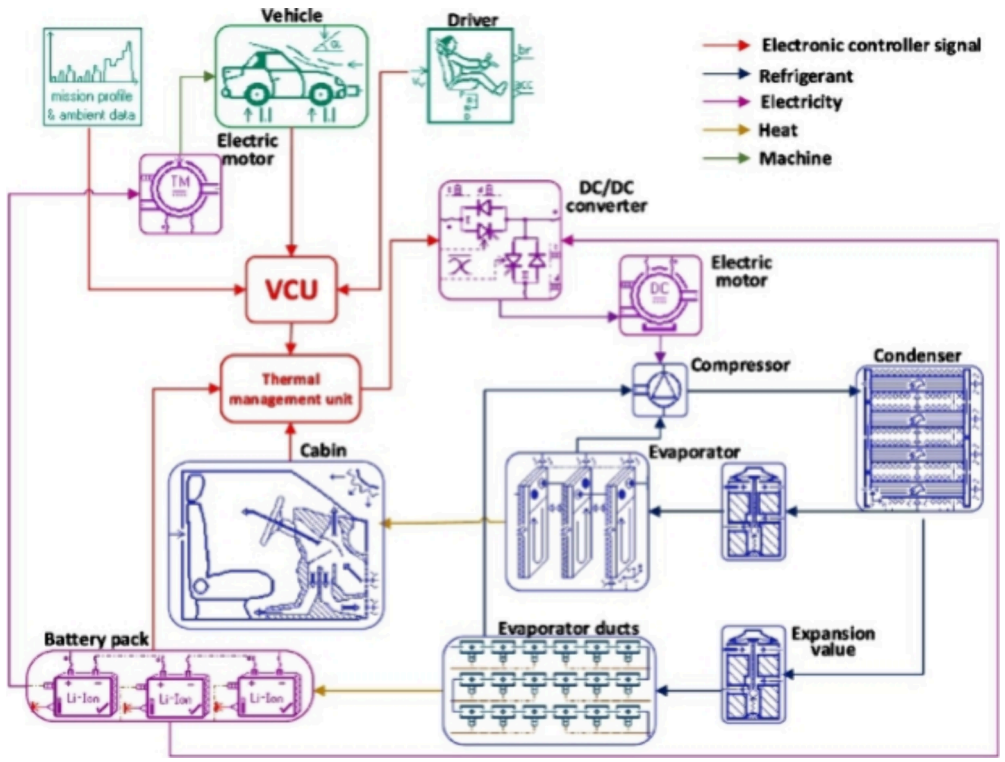



**Figure 10.** Schematic diagram of cold plate indirect cooling based on refrigerant.[115] Reprinted with permission from ref 115. Copyright 2020 Elsevier.



https://doi.org/10.1021/acsomega.4c02902
ACS Omega 2024, 9, 25591−25609

$$\overline{v}_m = \sum_{k=1}^{n} \alpha_k \rho_k \overline{v}_k \Big/ \rho_m \tag{5}$$

$$\rho_m = \sum_{k=1}^{n} a_k \rho_k \tag{6}$$

where, $\rho_m$ is density, $\overline{v}_m$ is average mass flow rate. $\alpha_k$ represents the volume fraction of the $k$ phase.

Momentum equations:

$$\frac{\partial}{\partial t}(\rho_m \overline{v}_m) + \nabla(\rho_m \overline{v}_m^{\,2}) = -\nabla P_a + [\mu_m(\nabla \overline{v}_m + \nabla \overline{v}_m^{\,T})] + \rho_m g + F + \nabla \cdot \left( \sum_{k=1}^{n} \alpha_k \rho_k \overline{v}_{d,k}^{\,2} \right) \tag{7}$$

$$\mu_m = \sum_{k=1}^{n} \alpha_k \mu_k \tag{8}$$

$$\overline{v}_{d,k} = \overline{v}_k - \overline{v}_m \tag{9}$$

where $F$ is body force, $P_a$ is pressure. $\mu$ is viscosity. $V_{d,k}$ is the $k$-phase slip velocity.

Energy equations:

$$\frac{\partial}{\partial t}\left( \sum_{k=1}^{n} \alpha_k \rho_k E_k \right) + \nabla \cdot \sum_{k=1}^{n} [\alpha_k \overline{v}_k (\overline{v}_k E_k + P)] = \nabla \cdot (k_{eff} \nabla T) + S_E \tag{10}$$

$$\overline{m}_{lv} = \frac{r \alpha_l \rho_l (T_l - T_{sat})}{T_{sat}} \quad T_l \geq T_{sat} \tag{11}$$

$$\overline{m}_{vl} = \frac{r \alpha_v \rho_v (T_v - T_{sat})}{T_{sat}} \quad T_v \leq T_{sat} \tag{12}$$

$$S_E = h_{fg} \overline{m} \tag{13}$$

where $k_{eff}$ is effective thermal conductivity. $\overline{m}_{lv}$ and $\overline{m}_{vl}$ are the evaporation and condensation mass transfer rate, respectively. $r$ is the phase transition mass transfer factor. $S_E$ is source item, and $h_{fg}$ is latent heat.

Two-phase volume fraction equation is

$$\frac{\partial}{\partial t}(a_p \rho_p) + \nabla(a_p \rho_p \overline{v}_m) = -\nabla(a_p \rho_p \overline{v}_{p,q}) \tag{14}$$

where $\alpha_p$ and $\alpha_q$ are volume fractions of the first and second phase, respectively. $\rho_p$ and $\rho_q$ are densities of the first and second phase, respectively. $\overline{v}_{p,q}$ is the relative velocity. The two-phase flow and heat transfer problems can be solved by using the above governing equations. It provides a theoretical basis for cold plate design and flow control optimization.

*3.2.1. Design Optimization.* The different structures and fluid flow forms of the cold plate mainly affect the pressure at the inlet and outlet of the cold plate and temperature distribution. Researchers[117−121] optimize the channel structure of R134a cooling, as shown in Figures 11 and 12, and simulate a coordinated control method involving the inlet flow rate and the evaporative pressure. This shows that by concurrently regulating the pressure and flow rate of the refrigerant, it is possible to effectively mitigate temperature elevation and achieve a balanced temperature distribution. In addition, the design and evaluation of refrigerant heat management

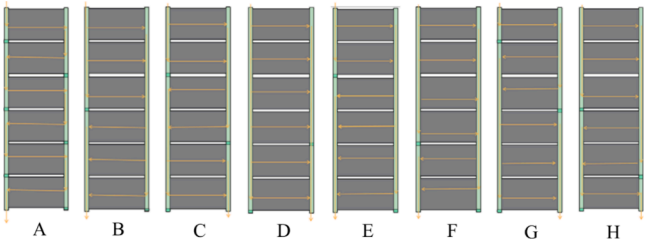



**Figure 11.** Diagram of refrigerant flow pattern.[117] Reprinted with permission from ref 117. Copyright 2021 Wiley.

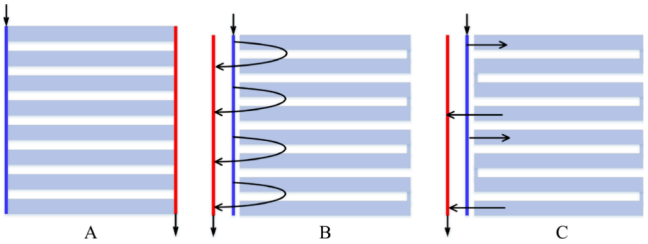



**Figure 12.** Inner layout of the cold plate.[121] Reprinted with permission from ref 121. Copyright 2019 Elsevier.

structures based on verified fluid−solid coupling models, as well as characteristic parameter analysis and control under diverse conditions, are discussed.[118] The optimal Type G is identified, demonstrating a modest pressure differential of 1670.6 Pa and achieving the highest heat-transfer coefficient of 810.8 W/(m$^2$·K). These results demonstrate that an optimal refrigerant mass flow rate solution exists for effective thermal management. A strategy prioritizing battery temperature reduction and temperature uniformity based on refrigerant characteristics is proposed. Researchers[120,121] confirm that vapor−liquid two-phase flow not only ensures the battery optimal working temperature but also improves the module temperature uniformity. Cen et al.[122] integrated the BTMS based on R134a with AC system and discussed its temperature control capability under extreme environments and road conditions. After confirming the exceptional properties of BTMS, Shen et al.[115] propose and analyze a new BTMS based on R134a, especially for high environment temperatures and high-speed dynamic working conditions. The results demonstrate effective control over the average temperature of the battery and the TD between individual batteries. It is also combined with the AC system, prioritizing the driver cabin control strategy and optimizing the target temperature control and system energy consumption.

In addition, a new design has been proposed by the study,[123] which consists of a metal honeycomb structure where the battery module is installed, and refrigerant flows through the honeycomb internal tube structure to cool the battery module. As shown in Figure 13, pipes are embedded in an aluminum block containing the battery and liquefied R290 boils inside the pipes. The aluminum block transfers the heat from the battery to the refrigerant, which undergoes a phase change inside the pipes. The advantage of this system is to prevent direct contact between R290 and the battery, reduce the temperature of the battery module and the TD among each battery, and reduce the amount of R290 used. Results show that at a discharge rate of 6C, the maximum battery temperature is 1 °C higher than that cooled by immersion in R290, and the maximum battery TD is 6.5 °C lower than that cooled by immersion in R290.



https://doi.org/10.1021/acsomega.4c02902
ACS Omega 2024, 9, 25591−25609

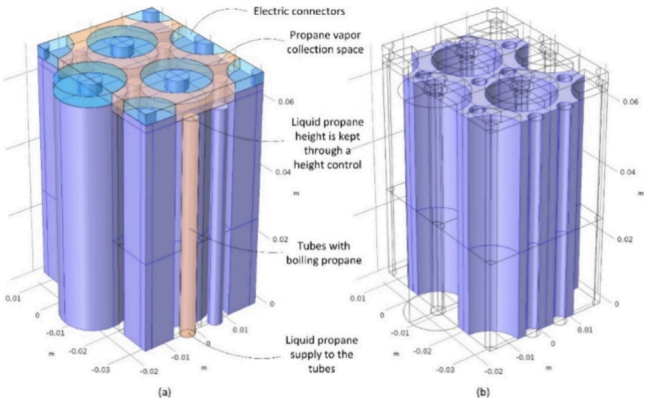



**Figure 13.** Schematic diagram of the batteries and the boiling R290 tubes:[123] (a) Integral structure. (b) Metal honeycomb structure. Reprinted with permission from ref 123. Copyright 2019 Elsevier.

Although refrigerant cooling has a strong cooling capacity and is less affected by ambient temperature, the working process of the system consumes a high amount of energy. In conditions of low environment temperature or minimal battery cooling requirements, using refrigerant cooling may result in a rapid decrease in battery temperature. Consequently, the compressor needs to frequently start and stop in order to keep the battery temperature within the desired range. However, frequent cycling of the compressor can potentially have a negative impact on its service life. Based on the previously information, some studies have proposed a new cooling scheme, which uses refrigerant cooling (R134a) and coolant (50% ethylene glycol solution) in parallel to cool the battery and has conducted relevant research on alternate cooling methods.[124−126] The schematic diagram is shown in Figure 14, and the allocation of the heat transfer area of the refrigerant pipeline and liquid cooling pipeline at the bottom of the battery is studied. Through a simulation system verification, the transient cooling process is investigated under various environment temperatures, compressor rotational speeds, and coolant flow rate. The results indicate that cooling with refrigerant and coolant simultaneously have a better effect compared with using refrigerant alone for cooling purposes. Then, in constant temperature mode, different strategies of controlling coolant flow rate are compared. The results indicate that the dual flow medium system had better temperature uniformity. The maximum energy savings in this mode is 49.15%.[125]

*3.2.2. Simulation and Experiment.* Temperature control of the cold plate indirect cooling technology with refrigerant is one of the crucial factors to ensure the battery safety and lifespan.[127] Currently, commonly used temperature control methods include constant temperature control and dynamic control. The constant temperature control method keeps the temperature of the refrigerant circulation system within a fixed range, thus ensuring stable operation of the battery. The dynamic control method adjusts the refrigeration capacity of the refrigerant circulation system based on the actual temperature changes on the battery surface, achieving fine BTM.

In research, numerical simulation and experimental validation are commonly used methods. Researchers can use computational fluid dynamics (CFD) software to proceed with numerical simulations of cold plate indirect cooling systems based on refrigerant to predict refrigerant flow and temperature distribution, thus determining the optimal design and control strategies for the refrigeration system.[117−119] In addition, simulation has characteristics of timeliness and convenience, and it can be reproduced in time in the face of new structures and new ideas. The above-mentioned literature studies use simulation methods to simulate and analyze new structures and mixed cooling methods.[124−126] Figure 15 shows the pipe layout and temperature distribution of an EV battery module refrigerant cooling system based on CFD simulation, using R134a and a transient VOF method.[128] By optimization of the layout of the refrigeration system and the refrigerant flow, the battery temperature can be obviously reduced. Furthermore, the performance of the BTMS is studied in terms of the effects of the initial temperature, flow rate, saturation temperature, thermal conductivity, and latent heat of the refrigerant. When the internal temperature of the battery module is too high, the AC system may initiate refrigerant circulation and deliver refrigerant into the battery module cold plate to dissipate heat. When the internal temperature of the battery module decreases to a certain degree, the AC system may automatically turn off the refrigerant circulation.

Experimental validation is also an important means of studying the performance and reliability of refrigeration

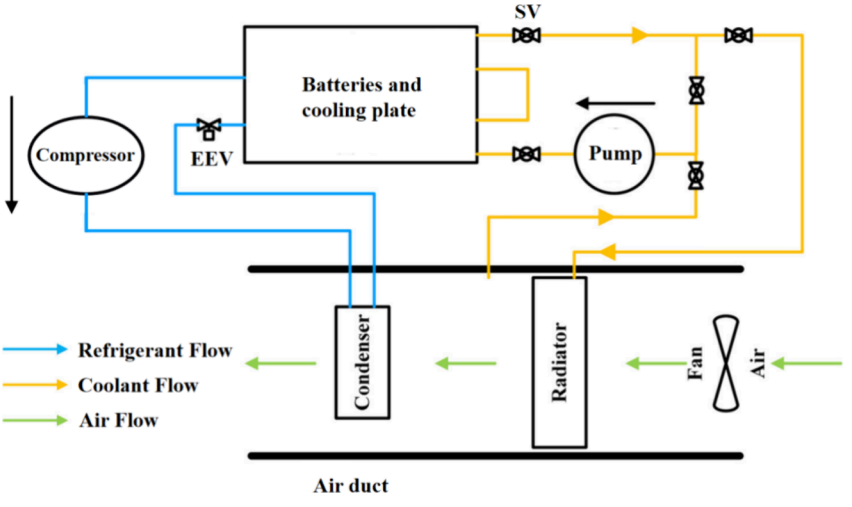



**Figure 14.** Schematic diagram of dual fluid medium system.[125] Reprinted with permission from ref 125. Copyright 2022 Elsevier.


https://doi.org/10.1021/acsomega.4c02902
ACS Omega 2024, 9, 25591−25609

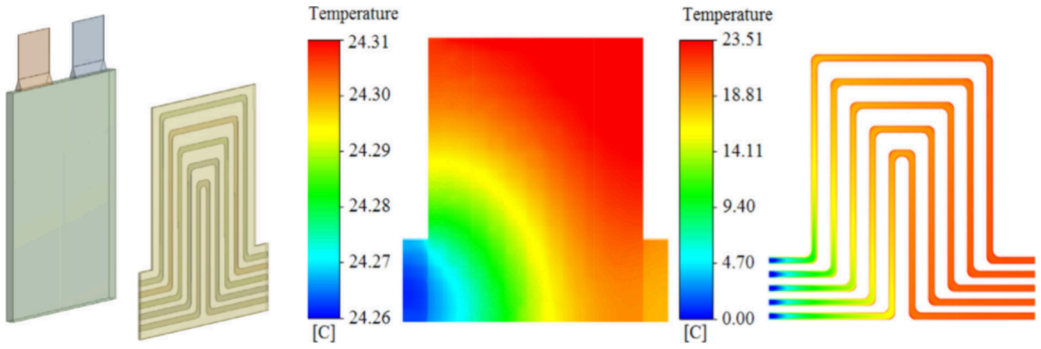



**Figure 15.** Pipe layout and temperature distribution.[128] Reprinted with permission from ref 128. Copyright 2022 Elsevier.

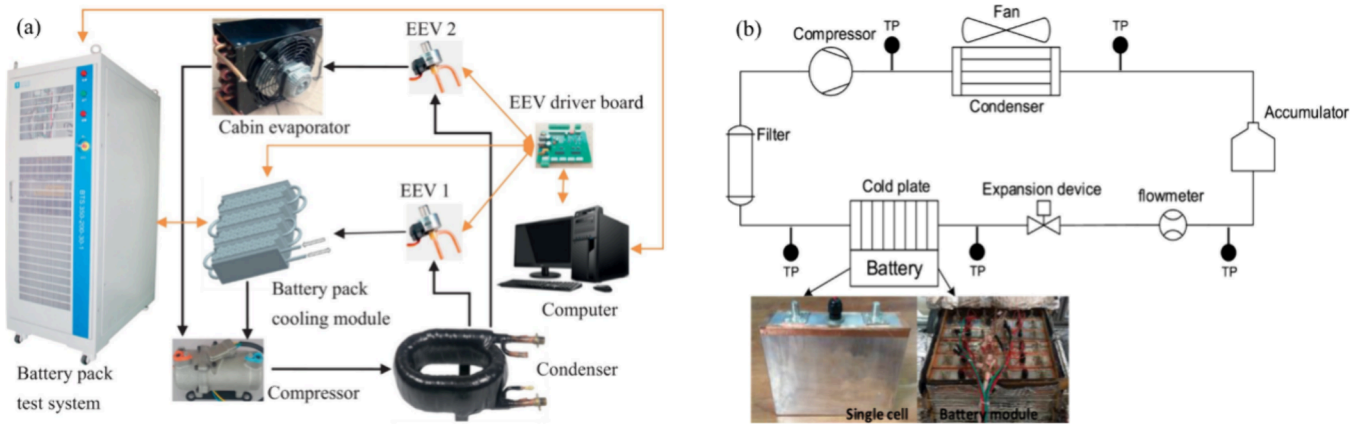



**Figure 16.** Experimental equipment for cold plate indirect cooling based on refrigerant: (a) With passenger cabin.[122] Photograph courtesy of Cen et al. Reprinted with permission from ref 122. Copyright 2018 Elsevier. (b) Without passenger cabin.[119] Photograph courtesy of Shen et al. Reprinted with permission from ref 119. Copyright 2020 Elsevier.

**Table 6. Indirect Cooling Main Research Content Summary**

| sources | battery | working condition | refrigerant | focus | results | method |
|---|---|---|---|---|---|---|
| 112 | Cylindrical battery | 100−200 W | R134a | Refrigerant charging amount and throttle opening | The throttle is open in 48.8−72.1%; the battery temperature can be controlled in the 10−45 °C range. | Experiment |
| 115 | $LiFeO_4$ 60 Ah | varying duty | R134a | Improve vehicle performance | The average temperature of the battery module is effectively controlled. | Simulation |
| 117−119 | NMC 94 Ah 3.7 V | 1C 2C 3C | R134a | Plate structure and flow property | Type G has a modest pressure difference of 1670.6 Pa and the highest heat-transfer coefficient of 810.8 W/($m^2$·K). | Experiment/ simulation |
| 122 | NCA 18650 2.2 Ah 3.6 V | 0.5C 1C 1.5C | R134a | Finned-tube heat exchanger and special aluminum frame | At a constant discharge rate, the temperature difference inside the battery pack is less than 4 °C. | Experiment |
| 123 | Cylindrical battery | 4C 6C | R290 | Honeycomb internal pipe structure | The maximum temperature difference is only 3.5 °C. | Simulation |
| 124−126 | NCM 94 Ah | 480 W | R134a and coolant | Dual flow medium system (DFMS) | The power consumption of the DFMS can be saved by 36.51%. | Experiment/ simulation |
| | | 192 W | | | | |
| 128 | Pouch battery 25 Ah 3.8 V | 3C | R134a | A direct evaporation cooling | Direct evaporation cooling could significantly reduce the maximum temperature. | Simulation |

systems. Researchers used an AC system to directly deliver refrigerants to the battery cooling system and verify the performance and reliability of the refrigeration system by testing. Huang et al.[112] conducted experimental studies on factors such as refrigerant charge amount, throttle valve opening, and heating power, and found that the refrigerant charge amount has an initial positive effect on system performance but then decreases. In addition, as the throttle valve opening increases, the heat transfer coefficient of the microchannel initially rises, reaches a stable state, and then plateaus. Similarly, as the heating power increases, the heat transfer coefficient initially rises, followed by a subsequent decline. When the generating heat power is 100−200 W, the battery working temperature can be controlled in a proper range by adjusting the throttle valve in the range of 48.8%−72.1%. Figure 16(a)[122] shows an experimental device for an EV battery cooling system, which adopts a fin-tube heat exchanger structure along with a specialized aluminum frame. The thermal management module of the cylindrical battery is designed to evaluate the performance and effectiveness of the refrigeration system by measuring parameters such as the battery temperature, the flow rate, the refrigerant temperature, etc. By optimizing the refrigerant circuit, the temperature nonuniformity inside the battery module can be diminished.


https://doi.org/10.1021/acsomega.4c02902
ACS Omega 2024, 9, 25591−25609

Figure 16(b)[119] ignores the passenger cabin, and the refrigerant flows directly into the four-inlets-four-outlets battery cold plate. The dummy battery is used to simulate the actual battery heat generation, and the average temperature of the battery module and cold plate of the system is measured under different discharge rates, environment temperatures, and mass flow rates to provide a reliable basis for numerical simulation. Table 6 summarizes the main research topics of indirect cooling.

Cold plate indirect cooling based on refrigerant has been applied to BTM for EVs. At present, some original equipment manufacturers (OEMs) of EVs have adopted the refrigerant direct cooling through a cold plate. This approach aims to improve the thermal dissipation capabilities and extend the operational lifespan of the battery[30] while also continuously optimizing and improving the technology. Starting from 2014, the BMW i-series battery electric vehicles (BEVs) have gradually adopted the cold plate indirect cooling based on a refrigerant, as shown in Table 7 (partial). The BYD Dynasty-series and Ocean-series have also gradually introduced refrigerant cooling models, especially the plug-in hybrid electric vehicles (PHEVs), which have both an engine and a battery module. Due to the compact space layout, the refrigerant cooling method with a simple structure and cost-saving advantage has been widely used.

**Table 7. Cold Plate Indirect Cooling of NEVs**

| OEMs | products | refrigerant | classification |
|---|---|---|---|
| BMW | i3 | R134a | BEV |
| BMW | X3 | R1234yf | PHEV |
| BMW | Mini | R1234yf | PHEV |
| Jeep | Compass | R1234yf | PHEV |
| BYD | Dolphin | R134a | BEV |
| BYD | Song-dmi | R134a | PHEV |
| BYD | Han-dmi | R134a | PHEV |

Taking the BYD Dolphin as an example, the Dolphin utilizes a wide-temperature-range and highly efficient heat pump system to reduce energy transfer stages and enhance energy utilization efficiency. The cold plate adopts a harmonica tube design combined with skinning, resembling a large flat panel. The entire cold plate consists of 8 cooling pipelines: 4 inlet pipelines and 4 outlet pipelines, arranged in a crisscross manner. Each pipeline is further divided into 30 units. There are total 240 flow channels in the plate, effectively enhancing heat transfer, employing a single inlet and single outlet circuit. Refrigerant is transported to the cold plate inlet through the AC pipe. The refrigerant is evaporated after absorbing the battery heat, and it converges into a collector tube. Subsequently, the refrigerant vapor circulated through the refrigerant pipeline loop into the compressor for the next cycle. When connecting and fixing the cold plate to the battery pack enclosure, this is achieved through the skinning structure using mechanical fasteners. In the design, aluminum tubes are used for the refrigerant pipeline.

During the operation of vehicle AC systems, the temperature of the evaporator surface is lower than the ambient ambient temperature, leading to the formation of condensation water. Condensation water is primarily generated in environments with significant temperature or humidity variations.[129] Condensation water forms when the water vapor in the air cools and then transitions into liquid water. In this BTMS, the cold plate acts as the evaporator.[115] The generation of condensation water inside the battery pack primarily depends on the environmental temperature, humidity, and design and sealing performance of the battery pack. As the refrigerant flows through the cold plate within the battery pack, it absorbs heat and facilitates cooling. This process may result in a decrease in the surface temperature of the battery pack. In scenarios with elevated environmental humidity, the cold plate surface may reach the dew point temperature. Consequently, under such circumstances, some condensation water could potentially form on the cold plate surface.

Nevertheless, with the increasing widespread application of BTMS utilizing cold plate indirect cooling methods with refrigerants in EVs, the design and fabrication of battery packs are becoming more mature. In general, an EV battery pack typically integrates a series of components, including battery modules, cold plate, positive temperature coefficient (PTC) heating film, pipelines, wiring, circuit boards, and more. In the design and manufacturing process of modern EV battery packs, efforts are often made to prevent external environmental moisture from entering the battery pack to ensure the normal operation and safety of the batteries.[130,131] The interior of the battery pack is maintained as an isolated and sealed space to prevent the impact of external environmental factors. It is designed to function under varying temperature and humidity conditions, making the occurrence of condensation water under normal circumstances highly unlikely.[132]

Therefore, in most conventional cases, it should be well-controlled and not have a significant impact on the performance and safety of the battery pack.

## 4. CONCLUSIONS

Based on a comprehensive review and summary, the design and application of a battery thermal management system (BTMS) based on refrigerant cooling with refrigerant as the core are introduced in this paper. This paper consolidates and extrapolates two prospective avenues for future development:

(1) Refrigerant cooling, with the sole working medium in electric vehicle (EV) of BTMS, varies in its physical and chemical properties based on different refrigerants, consequently affecting the refrigeration performance. Presently, research on refrigerant replacement primarily focuses on vehicle air conditioning (AC) systems. Compared with R134a, R1234yf and R152a have the advantage of smaller charge amounts. R744 cannot be directly charged into R134a-based vehicle AC systems due to its high exit pressure and the requirement of transcritical operation. Novel mixed refrigerants may combine the advantages of individual refrigerants. Yet, it is crucial to note that mixed refrigerants, due to differences in the boiling points of each single refrigerant, may experience temperature glide phenomena, necessitating precise control and experimental research. Studies focusing on mixtures application in vehicle AC system indirectly shed light on the performance of relevant refrigerants, offering guidance for BTMS. Additionally, the performance and thermodynamic characteristics of non-azeotropic and zeotropic mixed refrigerants represent a prominent research area, providing new alternative refrigerants for refrigerant cooling in BTMS.


https://doi.org/10.1021/acsomega.4c02902
ACS Omega 2024, 9, 25591−25609

(2) Immersion cooling utilizes boiling heat transfer with high efficiency. However, it necessitates stable pressure vessels to modulate refrigerant boiling temperature for improving temperature control. Coordinated control strategies involving temperature and refrigerant flow adjustment on demand represent crucial areas for future exploration. Cold plate indirect cooling, notably superior in heat exchange capabilities compared with liquid cooling, enhances adaptability to extreme temperature fluctuations. However, it is vital to optimize the cold plate design, inlet flow rate, and refrigerant evaporation pressure for influencing battery temperature and minimizing flow resistance.

The selection of refrigerants directly impacts the cooling performance. AC studies indirectly guide BTMS. Single refrigerants face the problem of environmental protection and cost. Mixed refrigerants reduce GWP and flammability issues, enhancing the system efficiency. Further research on mixed refrigerants is essential. Immersion cooling influences temperature control via the vessel pressure. Coordinated control strategies are crucial for cold plate indirect cooling, offering ongoing research prospects for optimizing plate design and smart controls.

## AUTHOR INFORMATION


### Corresponding Authors

**Yunpeng Hu** − *Department of Building Environment and Energy Engineering, Wuhan Business University, Wuhan 430056, China*; Email: yunpenghu@wbu.edu.cn

**Chunhua Zhang** − *Key Laboratory of Shaanxi Province for Development and Application of New Transportation Energy, Chang'an University, Xi'an 710064, China*; orcid.org/0000-0002-0349-390X; Email: zchzzz@126.com

### Authors

**Yujia Kang** − *Key Laboratory of Shaanxi Province for Development and Application of New Transportation Energy, Chang'an University, Xi'an 710064, China*; orcid.org/0000-0003-1837-3086

**Ke Yang** − *Key Laboratory of Shaanxi Province for Development and Application of New Transportation Energy, Chang'an University, Xi'an 710064, China*

**Quan Zhang** − *Key Laboratory of Shaanxi Province for Development and Application of New Transportation Energy, Chang'an University, Xi'an 710064, China*

Complete contact information is available at: https://pubs.acs.org/10.1021/acsomega.4c02902


### Notes

The authors declare no competing financial interest.

## ACKNOWLEDGMENTS

This study was supported by the Knowledge Innovation Program of Wuhan-Basic Research (2022010801010424), the Innovation Capability Support Program of Shaanxi (2021TD-28), and the Special Fund for Basic Scientific Research of Central Colleges, Chang'an University (300102222502, 300102383501, 300102383502).

## ABBREVIATIONS

### Greek symbols

$\alpha$, Volume fraction
$C_p$, Specific heat (J/(kg·K))
$E_0$, Operating voltage (V)
$F$, Body force
$h_{fg}$, Latent heat of vaporization (J/kg)
$I$, Current (A)
$k_b$, Thermal conductivity (W/(m·K))
$k_{eff}$, Effective heat transfer rate
$\overline{m}_{lv}$, Evaporation mass transfer rate (kg/(m$^3$·s))
$\overline{m}_{vl}$, Condensation mass transfer rate (kg/(m$^3$·s))
$\rho$, Density (kg/m$^3$)
$P$, Heat generation power (W)
$P_a$, Pressure (Pa)
$Q$, Heat generation (J)
$q$, Volume heat rate (W/m$^3$)
$r$, Phase transition mass transfer factor (s$^{-1}$)
$R_i$, Internal resistance ($\Omega$)
$S_E$, Source item
$T$, Temperature (K)
$\mu$, Viscosity (kg/(m·s))
$U$, Open circuit voltage (V)
$V$, Volume (m$^3$)
$\overline{v}_{d.\,k}$, $k$-phase slip velocity (m/s)
$\overline{v}_m$, Average mass flow rate (kg/s)
$\overline{v}_{p,\,q}$, Relative velocity between two phases

### Subscripts

$b$, Battery
$c$, Cooling
$m$, Mixed refrigerant
$l$, Liquid
$v$, Vapor
sat, Saturation

### Acronyms

AC, Air conditioning
BEV, Battery electric vehicle
BTM, Battery thermal management
BTMS, Battery thermal management system
CFCs, Chlorofluorocarbons
CFD, Computational fluid dynamics
COP, Coefficient of performance
DFMS, Dual flow medium system
EEV, Electronic expansion valve
EV, Electric vehicle
GWP, Global warming potential
HCs, Hydrocarbons
HCFCs, Hydrochlorofluorocarbons
HCFOs, Hydrochlorofluoroolefins
HFCs, Hydrofluorocarbons
HFOs, Hydrofluoroolefins
HP, Heat pump
LEL, Lower explosion limit
NEV, New energy vehicle
ODP, Ozone depletion potential
OEM, Original equipment manufacturer
PCM, Phase change material
PFCs, Perfluorocarbons
PHEV, Plug-in hybrid electric vehicles
PTC, Positive temperature coefficient
SOC, State of charge
TD, Temperature difference
TMS, Thermal management system


https://doi.org/10.1021/acsomega.4c02902
ACS Omega 2024, 9, 25591−25609

## REFERENCES


(1) Yang, A.-S.; Cai, T.-Y.; Su, L.; Li, Y.-S.; He, F.-F.; Zhang, Q.-P.; et al. Review on organic phase change materials for sustainable energy storage. *Sustainable Energy Fuels* **2022**, *6* (22), 5045−5071.

(2) Borowski, P.-F. Mitigating climate change and the development of green energy versus a return to fossil fuels due to the energy crisis in 2022. *Energies* **2022**, *15* (24), 9289.

(3) Zakeri, B.; Paulavets, K.; Barreto-Gomez, L.; Echeverri, L.-G.; Pachauri, S.; Boza-Kiss, B.; et al. Pandemic, war, and global energy transitions. *Energies* **2022**, *15* (17), 6114.

(4) Zhao, F.; Liu, X.; Zhang, H.; Liu, Z.-W. Automobile industry under China's carbon peaking and carbon neutrality goals: Challenges, opportunities, and coping strategies. *J. Adv. Transp.* **2022**, *2022*, 5834707.

(5) Wei, Y.-M.; Chen, K.-Y.; Kang, J.-N.; Chen, W.-M.; Zhang, X.-Y.; Wang, X.-Y. Policy and management of carbon peaking and carbon neutrality: A literature review. *Engineering* **2022**, *14*, 52−63.

(6) Song, D.-D.; Jia, B.-Y.; Jiao, H.-T. Review of renewable energy subsidy system in China. *Energies* **2022**, *15* (19), 7429.

(7) Kang, Y.-J.; Zhang, C.-H.; Yang, K.; Gao, Q. Analysis of the temperature change of a single battery based on Simulink. *Int. J. Electrochem. Sci.* **2021**, *16* (10), 21107.

(8) Ma, Y.; Yang, H.; Zuo, H.-Y.; Zuo, Q.-S.; He, X.-X.; Chen, W.; et al. EG@Bi-MOF derived porous carbon/lauric acid composite phase change materials for thermal management of batteries. *Energy* **2023**, *272*, 127180.

(9) E, J.-Q.; Qin, Y.-S.; Zhang, B.; Yin, H.-C.; Tan, Y. Effects of heating film and phase change material on preheating performance of the lithium-ion battery pack with large capacity under low temperature environment. *Energy* **2023**, *284*, 129280.

(10) Ma, Y.; Wei, R.-R.; Zuo, H.-Y.; Zuo, Q.-S.; Chen, Y.; Wu, S.-Y.; et al. Development of hierarchical MOF-based composite phase change materials with enhanced latent heat storage for low-temperature battery thermal optimization. *Energy* **2023**, *283*, 129001.

(11) Ren, R.-Y.; Zhao, Y.-H.; Diao, Y.-H.; Liang, L. Experimental study on the bottom liquid cooling thermal management system for lithium-ion battery based on multichannel flat tube. *Appl. Therm. Eng.* **2023**, *219*, 119636.

(12) Ma, Y.; Wei, R.-R.; Zuo, H.-Y.; Zuo, Q.-S.; Luo, X.-Y.; Chen, Y.; et al. N-doped EG@MOFs derived porous carbon composite phase change materials for thermal optimization of Li-ion batteries at low temperature. *Energy* **2024**, *286*, 129637.

(13) Ghaeminezhad, N.; Wang, Z. S.; Ouyang, Q. A review on lithium-ion battery thermal management system techniques: A control-oriented analysis. *Appl. Therm. Eng.* **2023**, *219*, 119497.

(14) Nazar, M.-W.; Iqbal, N.; Ali, M.; Nazir, H.; Amjad, M.-Z.-B. Thermal management of Li-ion battery by using active and passive cooling method. *J. Energy Storage* **2023**, *61*, 106800.

(15) Ma, J.; Sun, Y.-F.; Zhang, S.-A. Experimental investigation on energy consumption of power battery integrated thermal management system. *Energy* **2023**, *270*, 126860.

(16) Wu, H.-M.; Niu, M.; Shao, Y.-K.; Wang, M.-X.; Li, M.-H.; Liu, X.; et al. Investigations of li-ion battery thermal management systems based on heat pipes: A review. *ACS Omega* **2024**, *9* (1), 97−116.

(17) Yates, M.; Akrami, M.; Javadi, A.-A. Analysing the performance of liquid cooling designs in cylindrical lithium-ion batteries. *J. Energy Storage* **2021**, *33*, 100913.

(18) Ma, Y.; Yang, H.; Zuo, H.-Y.; Ma, Y.; Zuo, Q.-S; Chen, Y.; et al. Three-dimensional EG@MOF matrix composite phase change materials for high efficiency battery cooling. *Energy* **2023**, *278*, 127798.

(19) Tang, Z.-G.; Ji, Y.-T.; Yu, P.-P.; Cheng, J. P. Investigation on the thermal management performance of a non-contact flow boiling cooling system for prismatic batteries. *J. Energy Storage* **2023**, *66*, 107499.

(20) Mei, N.; Xu, X.-M.; Li, R.-Z. Heat dissipation analysis on the liquid cooling system coupled with a flat heat pipe of a lithium-ion battery. *ACS Omega* **2020**, *5* (28), 17431−17441.

(21) Wang, M.-W; Teng, S.-Y.; Xi, H.; Li, Y.-Q. Cooling performance optimization of air-cooled battery thermal management system. *Appl. Therm. Eng.* **2021**, *195*, 117242.

(22) Akbarzadeh, M.; Kalogiannis, T.; Jaguemont, J.; Jin, L.; Behi, H.; Karimi, D.; et al. A comparative study between air cooling and liquid cooling thermal management systems for a high-energy lithium-ion battery module. *Appl. Therm. Eng.* **2021**, *198*, 117503.

(23) E, S.-X.; Cui, Y.-X.; Liu, Y.-X.; Yin, H.-C. Effects of the different phase change materials on heat dissipation performances of the ternary polymer Li-ion battery pack in hot climate. *Energy* **2023**, *282*, 128805.

(24) E, S.-X.; Liu, Y.-X.; Cui, Y.-X.; Wu, A.-J.; Yin, H.-C. Effects of composite cooling strategy including phase change material and cooling air on the heat dissipation performance improvement of lithium ion power batteries pack in hot climate and its catastrophe evaluation. *Energy* **2023**, *283*, 129074.

(25) Yi, F.; E, J.-Q.; Zhang, B.; Zuo, H.-Y.; Wei, K.-X.; Chen, J.-W.; et al. Effects analysis on heat dissipation characteristics of lithium-ion battery thermal management system under the synergism of phase change material and liquid cooling method. *Renewable Energy* **2022**, *181*, 472−489.

(26) Lakhotia, V. K.; Senthil Kumar, R. A Review on various types of battery thermal management systems. *J. Therm. Anal. Calorim.* **2023**, *148*, 12335.

(27) Zhou, R.; Chen, Y.-M.; Zhang, J.-W.; Guo, P. Research progress in liquid cooling technologies to enhance the thermal management of LIBs. *Mater. Adv.* **2023**, *4* (18), 4011−4040.

(28) Liu, J.-H.; Chen, H.; Huang, S.-L.; Jiao, Y.; Chen, M.-Y. Recent progress and prospects in liquid cooling thermal management system for lithium-ion batteries. *Batteries-Basel* **2023**, *9* (8), 400.

(29) Hong, S.-H.; Jang, D.-S.; Park, S.; Yun, S.; Kim, Y. Thermal performance of direct two-phase refrigerant cooling for lithium-ion batteries in electric vehicles. *Appl. Therm. Eng.* **2020**, *173*, 115213.

(30) Wang, J.-B.; Gao, S.; Zhu, J.-H.; Mao, J.-N. Thermal performance analysis and burning questions of refrigerant direct cooling for electric vehicle battery. *Appl. Therm. Eng.* **2023**, *232*, 121055.

(31) Zhao, G.; Wang, X.-L.; Negnevitsky, M.; Li, C.-J. An up-to-date review on the design improvement and optimization of the liquid-cooling battery thermal management system for electric vehicles. *Appl. Therm. Eng.* **2023**, *219*, 119626.

(32) Maiorino, A.; Cilenti, C.; Petruzziello, F.; Aprea, C. A review on thermal management of battery packs for electric vehicles. *Appl. Therm. Eng.* **2024**, *238*, 122035.

(33) Lin, B.-C.; Cen, J.-W.; Jiang, F.-M. A lightweight compact lithium-ion battery thermal management system integratable directly with EV air conditioning systems. *J. Therm. Sci.* **2022**, *31* (6), 2363−2373.

(34) Gao, Y.; Gao, Q.; Zhang, X.-W. Study on battery direct-cooling coupled with air conditioner novel system and control method. *J. Energy Storage* **2023**, *70*, 108032.

(35) Cheng, Y. Carbon derivatives-directed international supervision laws and regulations and carbon market mechanism. *Sustainability* **2022**, *14* (23), 16157.

(36) Yang, D.-Z.; Li, Y.; Xie, J. - J.; Wang, F. Research and application progress of transcritical $CO_2$ refrigeration cycle system: A review. *Int. J. Low-Carbon Technol.* **2022**, *17*, 245−256.

(37) Kumar, A.; Chen, M. R.; Hung, K.-S.; Liu, C.-C.; Wang, C. C. A comprehensive review regarding condensation of low-GWP refrigerants for some major alternatives of R-134a. *Processes* **2022**, *10* (9), 1882.

(38) Dogan, E.; Chishti, M. Z.; Karimi Alavijeh, N.; Tzeremes, P. The roles of technology and Kyoto Protocol in energy transition towards COP26 targets: Evidence from the novel GMM-PVAR approach for G-7 countries. *Technol. Forecasting Social Change* **2022**, *181*, 121756.

(39) Sovacool, B.-K.; Griffiths, S.; Kim, J.; Bazilian, M. Climate change and industrial F-gases: A critical and systematic review of developments, sociotechnical systems and policy options for reducing




https://doi.org/10.1021/acsomega.4c02902
*ACS Omega* 2024, 9, 25591−25609

synthetic greenhouse gas emissions. *Renew. Sust. Energy Rev.* **2021**, *141*, 110759.
(40) Nguyen, D. K.; Huynh, T.-L.-D.; Nasir, M.-A. Carbon emissions determinants and forecasting: Evidence from G6 countries. *J. Environ. Manage.* **2021**, *285*, 111988.
(41) Rogelj, J.; den Elzen, M.; Hoehne, N.; Fransen, T.; Fekete, H.; Winkler, H.; et al. Paris Agreement climate proposals need a boost to keep warming well below 2 °C. *Nature* **2016**, *534* (7609), 631−639.
(42) He, J.-K.; Li, Z.; Zhang, X.-L.; Wang, H.-L.; Dong, W.-J.; Du, E.-S.; et al. Towards carbon neutrality: A study on China's long-term low-carbon transition pathways and strategies. *Environ. Sci. Ecotechnol.* **2022**, *9*, 100134.
(43) Mona, Y.; Chaichana, C.; Suttakul, P.; Watanabe, W.-C.; Do, T.-A. Effect of halocarbon refrigerants as working fluid of the heat pipe for thermoelectric power generation. *Energy Rep.* **2022**, *8*, 882−887.
(44) Zou, S.-K.; Zhang, Q.; Yue, C.; Wang, J.-Q.; Du, S. Study on the performance and free cooling potential of a R32 loop thermosyphon system used in data center. *Energy Build.* **2022**, *256*, 111682.
(45) Kumma, N.; Kruthiventi, S.-S.-H. Current status of refrigerants used in domestic applications: A review. *Renewable Sustainable Energy Rev.* **2024**, *189*, 114073.
(46) Vuppaladadiyam, A.-K.; Antunes, E.; Vuppaladadiyam, S.-S.-V.; Baig, Z.-T.; Subiantoro, A.; Lei, G.-Y.; et al. Progress in the development and use of refrigerants and unintended environmental consequences. *Sci. Total Environ.* **2022**, *823*, 153670.
(47) Song, X.; Yuan, H.-R.; Zhang, Y.; Yu, B.-B.; Wang, D.-D.; Shi, J.-Y.; et al. Experimental study on improved performance of an automotive $CO_2$ air conditioning system with an evaporative gas cooler. *Int. J. Refrig.* **2022**, *140*, 39−48.
(48) Vuppaladadiyam, A. K.; Antunes, E.; Vuppaladadiyam, S. S. V.; Baig, Z. T.; Subiantoro, A.; Lei, G.; Leu, S.-Y.; Sarmah, A. K.; Duan, H. Progress in the development and use of refrigerants and unintended environmental consequences. *Sci. Total Environ.* **2022**, *823*, 153670.
(49) Shafiq, Q.-N.; Liaw, J.-S.; Wang, C.-C. A comprehensive review on the nucleate/convective boiling of low-GWP refrigerants: Alternatives to HFC refrigerants. *Processes* **2023**, *11* (2), 468.
(50) Wang, F.; You, T. Comparative analysis on the life cycle climate performance of ground source heat pump using alternative refrigerants. *Case Stud. Therm. Eng.* **2023**, *42*, 102761.
(51) Yang, Z.; Feng, B.; Ma, H.-Y.; Zhang, L.; Duan, C.-J.; Liu, B.; et al. Analysis of lower GWP and flammable alternative refrigerants. *Int. J. Refrig.* **2021**, *126*, 12−22.
(52) Zhang, X.-P.; Wang, F.-X.; Fan, W.; Xue, Y.-F. Binary blend of carbon dioxide and fluoro ethane as working fluid in transcritical heat pump systems. *Therm. Sci.* **2015**, *19* (4), 1317−1321.
(53) Dong, J.; Wang, Y.; Jia, S.; Zhang, X.-H.; Huang, L.-J. Experimental study of R744 heat pump system for electric vehicle application. *Appl. Therm. Eng.* **2021**, *183*, 116191.
(54) Wang, Y.-B.; Dong, J.-Q.; Jia, S.-W.; Huang, L.-J. Experimental comparison of R744 and R134a heat pump systems for electric vehicle application. *Int. J. Refrig.* **2021**, *121*, 10−22.
(55) Song, X.; Lu, D.; Lei, Q.; Wang, D.-D.; Yu, B.-B.; Shi, J.-Y.; et al. Energy and exergy analyses of a transcritical $CO_2$ air conditioning system for an electric bus. *Appl. Therm. Eng.* **2021**, *190*, 116819.
(56) Elbarghthi, A.-F.-A.; Hdaib, M.-Y.; Dvorak, V. Heat transfer analysis between R744 and HFOs inside plate heat exchangers. *Entropy* **2022**, *24* (8), 1150.
(57) Gao, Y.-P.; Shao, S.-Q.; Zhan, B.-F.; Chen, Y.-Y.; Tian, C.-Q. Heat transfer and pressure drop characteristics of ammonia during flow boiling inside a horizontal small diameter tube. *Int. J. Heat Mass Transfer* **2018**, *127*, 981−996.
(58) Jiang, L.; Wang, R.-Z.; Li, J.-B.; Wang, L.-W.; Roskilly, A.-P. Performance analysis on a novel sorption air conditioner for electric vehicles. *Energy Convers. Manage.* **2018**, *156*, 515−524.
(59) Xu, X.-L.; Qi, Y.-X.; Lu, Y.; Han, S.-K.; Yang, Y.-S.; Zhang, X.-Q.; et al. Experimental study on PVTx properties of a binary R1234yf/R152a refrigerant. *J. Chem. Eng. Data* **2022**, *67* (10), 2913−2919.
(60) Chen, X.-W.; Liang, K.; Li, Z.-H.; Zhao, Y.; Xu, J.; Jiang, H.-Y. Experimental assessment of alternative low global warming potential refrigerants for automotive air conditioners application. *Case Stud. Therm. Eng.* **2020**, *22*, 100800.
(61) Zhang, N.-C.; Dai, Y.-D.; Feng, L.-H.; Li, B. Study on environmentally friendly refrigerant R13I1/R152a as an alternative for R134a in automotive air conditioning system. *Chin. J. Chem. Eng.* **2022**, *44*, 292−299.
(62) Li, H.-P.; Tang, K. A comprehensive study of drop-in alternative mixtures for R134a in a mobile air-conditioning system. *Appl. Therm. Eng.* **2022**, *203*, 117914.
(63) Chen, X.-W.; Liang, K.; Li, Z.-H.; Jiang, H.-Y.; Xu, J. Energy and exergy analysis of domestic refrigerators using R152a to replace R134a. *Therm. Sci. Eng. Prog.* **2022**, *29*, 101235.
(64) Ma, J.; Sun, Y.-F.; Zhang, S.-A.; Li, J.; Li, S.-G. Experimental study on the performance of vehicle integrated thermal management system for pure electric vehicles. *Energy Convers. Manage.* **2022**, *253*, 115183.
(65) Direk, M.; Mert, M.-S.; Soylu, E.; Yüksel, F. Experimental investigation of an automotive air conditioning system using R444a and R152a refrigerants as alternatives of R134a. *Strojniski Vestnik-Journal of Mechanical Engineering.* **2019**, *65* (4), 212−218.
(66) Serevina, V.; Azhar, A.-A.; Sutandi, T.; Sumeru, K. Effect of engine speed on the performance of automotive air conditioning system using R134a and R152a as refrigerants. *J. Phys. Conf. Ser.* **2019**, *1150*, No. 012051.
(67) Lei, S.-R.; Guo, B.; Zhao, Z.-L. Exergy analysis of heat pump air conditioning systems for pure electric vehicle use with low-GWP refrigerants. *Int. J. Refrig.* **2023**, *156*, 266−277.
(68) Vaghela, J.-K. Comparative evaluation of an automobile air-conditioning system using R134a and its alternative refrigerants. International conference on recent advancement in air conditioning and refrigeration, RAAR 2016, 2017*109*153160
(69) Kang, Y.-J.; Zhang, C.-H.; Ma, J.; Yang, K. Numerical simulation of indirect contact phase-change cooling system with R1234yf/R152a mixed refrigerant for battery thermal management. *Energy Source Part A* **2023**, *45* (3), 9093−9117.
(70) Sumeru, K.; Sunardi, C.; Aziz, A.-A.; Nasution, H.; Abioye, A.-M.; Said, M.-F.-M. Comparative performance between R134a and R152a in an air conditioning system of a passenger car. *J. Teknol.* **2016**, *78*, 1−6.
(71) Ma, Z.-X.; Liu, F.-G.; Tian, C.-F.; Jia, L.-L.; Wu, W. Experimental comparisons on a gas engine heat pump using R134a and low-GWP refrigerant R152a. *Int. J. Refrig.* **2020**, *115*, 73−82.
(72) Al-Sayyab, A.-K.-S.; Navarro-Esbri, J.; Barragan-Cervera, A.; Kim, S.; Mota-Babiloni, A. Comprehensive experimental evaluation of R1234yf-based low GWP working fluids for refrigeration and heat pumps. *Energy Convers. Manage.* **2022**, *258*, 115378.
(73) Ojeda, F.-W.-A.-B.; Queiroz, M.-V.-A.; Pico, D.-F.-M.; Parise, J.-A.-D.; Bandarra, E.-P. Experimental evaluation of low-GWP refrigerants R513A, R1234yf and R436A as alternatives for R134a in a cascade refrigeration cycle with R744. *Int. J. Refrig.* **2022**, *144*, 175−187.
(74) Pham, Q.-V.; Oh, J.-T. Condensation heat transfer characteristics of R1234yf inside multiport mini-channel tube. *Int. J. Heat Mass Transfer* **2021**, *170*, 121029.
(75) Tasdemirci, E.; Alptekin, E.; Hosoz, M. Comparative performance of an automobile heat pump system with an internal heat exchanger using R1234yf and R134a. *Int. J. Exergy* **2020**, *33* (1), 98−113.
(76) Longo, G.-A.; Mancin, S.; Righetti, G.; Zilio, C. Saturated vapour condensation of R134a inside a 4 mm ID horizontal smooth tube: Comparison with the low GWP substitutes R152a, R1234yf and R1234ze(E). *Int. J. Heat Mass Transfer* **2019**, *133*, 461−473.


https://doi.org/10.1021/acsomega.4c02902
*ACS Omega* 2024, 9, 25591−25609

(77) Illan-Gomez, F.; Garcia-Cascales, J.-R. Experimental comparison of an air-to-water refrigeration system working with R134a and R1234yf. *Int. J. Refrig.* **2019**, *97*, 124−131.
(78) Zhao, Y.; Chen, J.; Xu, B.; He, B. Performance of R-1234yf in mobile air conditioning system under different heat load conditions. *Int. J. Air-Cond. Refrig.* **2012**, *20* (3), 1250016.
(79) Zhao, Y.; Qi, Z.; Chen, J.; Xu, B.; He, B. Experimental analysis of the low-GWP refrigerant R1234yf as a drop-in replacement for R134a in a typical mobile air conditioning system. *Proc. Inst. Mech. Eng., Part C: J. Mech. Eng. Sci.* **2012**, *226* (11), 2713−2725.
(80) Yu, B.-B.; Ouyang, H.-S.; Shi, J.-Y.; Guo, Z.-K.; Chen, J.-P. Experimental evaluation of cycle performance for new-developed refrigerants in the electric vehicle heat pump systems. *Int. J. Refrig.* **2021**, *129*, 118−127.
(81) Wu, X.; Yang, Z.; Liu, H.-W.; Huan, Z.-J.; Wang, W.-B. The performance of mixture refrigerant R134a/R152a in a novel gas engine-driven heat pump system. *Int. J. Green Energy* **2014**, *11* (1), 60−74.
(82) Yildiz, A.; Yildirim, R. Experimental investigation of exergy, exergoenvironmental and exergoenviroeconomic analysis of the heat pump system. *Int. J. Environ. Sci. Technol.* **2022**, *19* (11), 10737−10746.
(83) Bolaji, B.-O. Experimental study of R152a and R32 to replace R134a in a domestic refrigerator. *Energy* **2010**, *35* (9), 3793−3798.
(84) Abraham, J.-D.-A.-P.; Mohanraj, M. Thermodynamic performance of automobile air conditioners working with R430A as a drop-in substitute to R134a. *J. Therm. Anal. Calorim.* **2019**, *136* (5), 2071−2086.
(85) Xu, C.; Qian, Z.-Q.; Ren, J. A comprehensive experimental investigation of additives to enhance pool boiling heat transfer of a non-azeotropic mixture. *Entropy* **2022**, *24* (11), 1534.
(86) Deng, H.; Fernandino, M.; Dorao, C.-A. A numerical investigation of flow boiling of non-azeotropic and near-azeotropic binary mixtures. *Int. J. Refrig.* **2015**, *49*, 99−109.
(87) He, X.-J.; Wang, J.; Li, Z.-L.; Wan, R.; Hu, J.; Yang, Z.-M. Numerical simulation on shell-side flow pattern transition and heat transfer of non-azeotropic refrigerant mixture. *Appl. Therm. Eng.* **2022**, *214*, 118917.
(88) Xu, J.; Wang, Y.; Yang, R.; Liu, W.-L.; Wu, H.-W.; Ding, Y.-L.; et al. A review of boiling heat transfer characteristics in binary mixtures. *Int. J. Heat Mass Transfer* **2021**, *164*, 120570.
(89) Meng, Z.; Zhang, H.; Lei, M.; Qin, Y.-B.; Qiu, J.-Y. Performance of low GWP R1234yf/R134a mixture as a replacement for R134a in automotive air conditioning systems. *Int. J. Heat Mass Transfer* **2018**, *116*, 362−370.
(90) Lee, Y.; Kang, D.-G.; Jung, D. Performance of virtually non-flammable azeotropic HFO1234yf/HFC134a mixture for HFC134a applications. *Int. J. Refrig.* **2013**, *36*, 1203−1207.
(91) Shin, Y.; Kim, T.; Lee, A.; Cho, H. Performance characteristics of automobile air conditioning using the R134a/R1234yf mixture. *Entropy* **2020**, *22* (4), 1096.
(92) Sun, D.-H.; Zhang, X.; Liu, Z.-Y.; Zhang, H. Comparative study on boiling heat transfer characteristics and performance of low-temperature heating system of R744 and its azeotropic refrigerant. *Energies* **2023**, *16* (3), 1313.
(93) Zhao, Y.-X.; Li, Z.-B.; Zhang, X.-J.; Dong, X.-Q.; Gong, M.-Q. Prediction of ternary azeotropic refrigerants containing ammonia. *Int. J. Refrig.* **2021**, *131*, 101−108.
(94) Yancey, A.-D.; Corbin, D.-R.; Shiflett, M.-B. Difluoromethane (HFC-32) and pentafluoroethane (HFC-125) sorption on Linde type A (LTA) zeolites for the separation of azeotropic hydrofluorocarbon refrigerant mixtures. *Langmuir* **2022**, *38* (6), 1937−1953.
(95) Wang, L.-L.; Li, H.-X.; Wu, J.-H.; Qiu, K. Feasibility of using near-azeotropic refrigerant mixture R290/R1234ze(E) as substitute for R22. *Environ. Prog. Sustainable Energy* **2021**, *40* (3), e13574.
(96) Azzolin, M.; Berto, A.; Bortolin, S.; Del Col, D. Condensation heat transfer of R1234ze(E) and its A1 mixtures in small diameter channels. *Int. J. Refrig.* **2022**, *137*, 153−165.
(97) Kaniowski, R.; Pastuszko, R. Pool boiling experiment with Novec-649 in microchannels for heat flux prediction. *Exp. Therm Fluid Sci.* **2023**, *141*, 110802.
(98) Wu, N.; Ye, X.-L.; Yao, J.-X.; Zhang, X.; Zhou, X.-L.; Yu, B. Efficient thermal management of the large-format pouch lithium-ion cell via the boiling-cooling system operated with intermittent flow. *Int. J. Heat Mass Transfer* **2021**, *170*, 121018.
(99) Muszynski, T.; Mikielewicz, D. Comparison of heat transfer characteristics in surface cooling with boiling microjets of water, ethanol and HFE7100. *Appl. Therm. Eng.* **2016**, *93*, 1403−1409.
(100) Roe, C.; Feng, X.-N.; White, G.; Li, R.-H.; Wang, H. B.; Rui, X.-Y.; et al. Immersion cooling for lithium-ion batteries - a review. *J. Power Sources* **2022**, *525*, 231094.
(101) Van Gils, R.-W.; Danilov, D.; Notten, P.-H.-L.; Speetjens, M.-F.-M.; Nijmeijer, H. Battery thermal management by boiling heat-transfer. *Energy Convers. Manage.* **2014**, *79*, 9−17.
(102) Al-Zareer, M.; Dincer, I.; Rosen, M.-A. A novel approach for performance improvement of liquid to vapor based battery cooling systems. *Energy Convers. Manage.* **2019**, *187*, 191−204.
(103) Al-Zareer, M.; Dincer, I.; Rosen, M.-A. A thermal performance management system for lithium-ion battery packs. *Appl. Therm. Eng.* **2020**, *165*, 114378.
(104) Wang, Y.-F.; Wu, J.-T. Thermal performance predictions for an HFE-7000 direct flow boiling cooled battery thermal management system for electric vehicles. *Energy Convers. Manage.* **2020**, *207*, 112569.
(105) Wang, Y.-F.; Li, B.; Hu, Y.; Mao, Z.-Y.; Song, B.-W.; Tian, W.-L.; et al. Experimental study on immersion phase change cooling of lithium-ion batteries based on R1233ZD(E)/ethanol mixed refrigerant. *Appl. Therm. Eng.* **2023**, *220*, 119649.
(106) Zhao, R.; Liu, J.; Gu, J.-J.; Zhai, L.; Ma, F. Experimental study of a direct evaporative cooling approach for Li-ion battery thermal management. *Int. J. Energy Res.* **2020**, *44* (8), 6660−6673.
(107) Al-Zareer, M.; Dincer, I.; Rosen, M.-A. A novel phase change based cooling system for prismatic lithium ion batteries. *Int, J. Refrig.* **2018**, *86*, 203−217.
(108) Al-Zareer, M.; Dincer, I.; Rosen, M.-A. Development and evaluation of a new ammonia boiling based battery thermal management system. *Electrochim. Acta* **2018**, *280*, 340−352.
(109) Al-Zareer, M.; Dincer, I.; Rosen, M.-A. Heat and mass transfer modeling and assessment of a new battery cooling system. *Int. J. Heat Mass Transfer* **2018**, *126*, 765−778.
(110) Al-Zareer, M.; Dincer, I.; Rosen, M.-A. A thermal performance management system for lithium-ion battery packs. *Appl. Therm. Eng.* **2020**, *165*, 114378.
(111) Goodarzi, M.; Jannesari, H.; Ameri, M. Experimental study of Li-ion battery thermal management based on the liquid-vapor phase change in direct contact with the cells. *J. Energy Storage* **2023**, *62*, 106834.
(112) Huang, D.-Z.; Zhang, H.-Y.; Wang, X.-J.; Huang, X.-H.; Dai, H.-F. Experimental investigations on the performance of mini-channel evaporator refrigeration system for thermal management of power batteries. *Int. J. Refrig.* **2021**, *130*, 117.
(113) Fang, Y.-D.; Yang, W.-L.; Xu, D.; Hu, L.-R.; Su, L.; Huang, Y.-Q. Experimental investigation on flow boiling characteristics of R1233zd(E) in a parallel mini-channel heat sink for the application in battery thermal management. *Int. J. Heat Mass Transfer* **2021**, *178*, 121591.
(114) Yeo, I.; Lee, S. 2D computational investigation into transport phenomena of subcooled and saturated flow boiling in large length to diameter ratio micro-channel heat sinks. *Int. J. Heat Mass Transfer* **2022**, *183*, 122128.
(115) Shen, M.; Gao, Q. System simulation on refrigerant-based battery thermal management technology for electric vehicles. *Energy Convers. Manage.* **2020**, *203*, 112176.
(116) Chen, H.-P.; Zhang, T.-S.; Gao, Q.; Han, Z.-W.; Xu, Y.-H.; Yang, K.-Q.; et al. Advance and prospect of power battery thermal management based on phase change and boiling heat transfer. *J. Energy Storage* **2022**, *53*, 105254.


https://doi.org/10.1021/acsomega.4c02902
*ACS Omega* 2024, 9, 25591−25609

(117) Wang, Y.; Gao, Q.; Wang, H.-W. Structural design and its thermal management performance for battery modules based on refrigerant cooling method. *Int. J. Energy Res.* **2021**, *45* (3), 3821−3837.
(118) Wang, G.-H.; Gao, Q.; Yan, Y.-Y.; Zhang, Y.-X. Transient process optimization of battery cooling on heat transfer enhancement structure. *Appl. Therm. Eng.* **2021**, *182*, 115897.
(119) Shen, M.; Gao, Q. Structure design and effect analysis on refrigerant cooling enhancement of battery thermal management system for electric vehicles. *J. Energy Storage* **2020**, *32*, 101940.
(120) Li, X.-J.; Jia, L.; Dang, C.; An, Z.-J.; Huang, Q. Effect of flow instability on flow boiling friction pressure drop in parallel micro-channels. *Int. Commun. Heat Mass Transfer* **2018**, *97*, 64−71.
(121) Yan, Q.; Jia, L.; An, Z. J.; Peng, Q. A comprehensive criterion for slug-annular flow transition based on flow boiling of R134a in microchannels. *Int. Commun. Heat Mass Transfer* **2019**, *105*, 1−9.
(122) Cen, J.-W.; Li, Z.-B.; Jiang, F. M. Experimental investigation on using the electric vehicle air conditioning system for lithium-ion battery thermal management. *Energy Sustainable Dev.* **2018**, *45*, 88−95.
(123) Al-Zareer, M.; Dincer, I.; Rosen, M.-A. Development and analysis of a new tube based cylindrical battery cooling system with liquid to vapor phase change. *Int. J. Refrig.* **2019**, *108*, 163−173.
(124) Jin, S.; Gao, Q.; Gao, X.; Gao, Y.; Zhang, T.-S. Study on dual flow medium system for battery thermal management of electric vehicle. *Case Stud. Therm. Eng.* **2022**, *35*, 102023.
(125) Jin, S.; Gao, Q.; Zhang, T.-S. Experimental study on a novel battery cooling system containing dual flow medium. *Int. J. Heat Mass Transfer* **2022**, *199*, 123483.
(126) Jin, S.; Gao, Q.; Zhang, T.-S. Simulation of battery simultaneous cooling based on the dual fluid medium system. *J. Energy Storage* **2023**, *61*, 106732.
(127) Lu, M.-Y.; Zhang, X.-L.; Ji, J.; Xu, X.-F.; Zhang, Y. Research progress on power battery cooling technology for electric vehicles. *J. Energy Storage* **2020**, *27*, 101155.
(128) Wang, Z.-K.; Wang, Y.-A.; Xie, Z.-F.; Li, H.; Peng, W.-L. Parametric investigation on the performance of a direct evaporation cooling battery thermal management system. *Int. J. Heat Mass Transfer* **2022**, *189*, 122685.
(129) Xu, Z.-Y.; Wang, R.-Z. Air-conditioning and refrigeration: Current status and future perspectives. *Chinese Science Bulletin-Chinese* **2020**, *65* (24), 2555−2570.
(130) Ma, C.-C.; Hou, J.-H.; Lan, F.-C. Optimization analysis of power battery pack box structure for new energy vehicles. *Proceedings of the 3rd International Symposium on New Energy and Electrical Technology*; Springer, 2023; *1017*, pp 641−648.
(131) Kumar, R.; Goel, V. A study on thermal management system of lithium-ion batteries for electrical vehicles: A critical review. *J. Energy Storage* **2023**, *71*, 108025.
(132) Liao, C.-L.; Wang, J.-Y. Study on the influence of operating environment conditions on the performance of power lithium battery system. *2022 IEEE International Conference on Electrical Engineering, Big Data and Algorithms (EEBDA)*; IEEE, 2022; pp 688−692.


https://doi.org/10.1021/acsomega.4c02902
*ACS Omega* 2024, 9, 25591−25609